

This report has been reviewed by the RADC Information Office (OI) and is releasable to the National Technical Information Service (NTIS). The report will be releasable to the general public, including foreign nations.

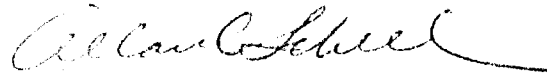
RADC-TR-79-21 has been reviewed and is approved for publication.

APPROVED:



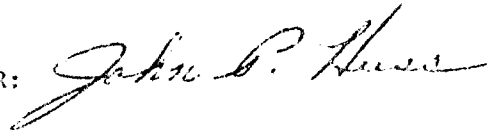
PHILIP BLACKSMITH
Branch Chief
Electromagnetic Systems Concepts Branch

APPROVED:



ALLAN C. SCHELL
Acting Chief
Electromagnetic Sciences Division

FOR THE COMMANDER:



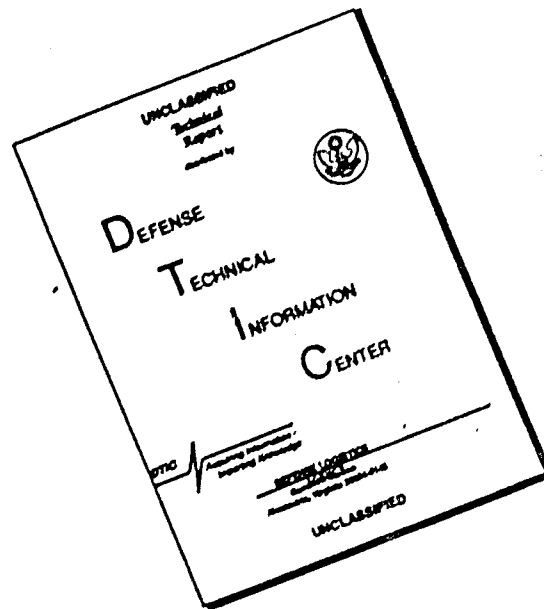
JOHN P. HUSS
Chief, Plans Office

If your address has changed or if you wish to be removed from the RADC mailing list, or if the addressee is no longer employed by your organization, please notify RADC (EEC), Hanscom AFB MA 01730. This will assist us in maintaining a current mailing list.

Do not return this copy. Retain or destroy.

BEST AVAILABLE COPY

DISCLAIMER NOTICE



THIS DOCUMENT IS BEST QUALITY AVAILABLE. THE COPY FURNISHED TO DTIC CONTAINED A SIGNIFICANT NUMBER OF PAGES WHICH DO NOT REPRODUCE LEGIBLY.

UNCLASSIFIED

SECURITY CLASSIFICATION OF THIS PAGE (When Data Entered)

9070

19 REPORT DOCUMENTATION PAGE		READ INSTRUCTIONS BEFORE COMPLETING FORM	
1. REPORT NUMBER RADC-TR-79-714	2. GOVT ACCESSION NO.	3. RECIPIENT'S CATALOG NUMBER 9 Interim rept.	
4. TITLE (and Subtitle) SCATTERING FROM OBSTACLES OVER THE EARTH		5. TYPE OF REPORT & PERIOD COVERED Interim Report Scientific Report No. 1	
7. AUTHOR(s) R. W. P. King, H. M. Lee L. C. Shen		8. CONTRACT OR GRANT NUMBER(s) F19628-77-C-01462/	
6. PERFORMING ORGANIZATION NAME AND ADDRESS Gordon McKay Laboratory Division of Applied Sciences, Harvard University Cambridge MA 02138		10. PROGRAM ELEMENT, PROJECT, TASK AREA & WORK UNIT NUMBERS 61102F 23051426	
11. CONTROLLING OFFICE NAME AND ADDRESS Deputy for Electronic Technology (RADC/EEC) Hanscom AFB MA 01730		12. REPORT DATE Apr 1979	
14. MONITORING AGENCY NAME & ADDRESS (if different from Controlling Office) Same		13. NUMBER OF PAGES 54	
		15. SECURITY CLASS. (of this report) UNCLASSIFIED	
		15a. DECLASSIFICATION/DOWNGRADING SCHEDULE N/A	
16. DISTRIBUTION STATEMENT (of this Report) Approved for public release; distribution unlimited.			
14 SCIENTIFIC-1			
17. DISTRIBUTION STATEMENT (of the abstract entered in Block 20, if different from Report) Same			
18. SUPPLEMENTARY NOTES RADC Project Engineer: Otho E. Kerr (EEC)			
19. KEY WORDS (Continue on reverse side if necessary and identify by block number) Scattered fields from metal loops and horizontal wires over the earth Description of experimental equipment, design and results Theoretical treatment of driven Beverage antenna and horizontal wire as scatter, each with known current distributions. (E squared)			
20. ABSTRACT (Continue on reverse side if necessary and identify by block number) In PART I of this report the experimental setup and techniques for measuring the fields scattered from a metal circular loop and a straight wire placed above the ground are described. Measured scattered fields E^2 are presented as functions of loop size, the height of the loop above the ground, and the location of the receiving antenna. The frequency used was 1.5 GHz. Resonant and nonresonant loops and a straight wire a half wavelength long were used. The experiments were performed on an open ground with the scatterer placed less than a third of a wavelength above the ground. The relative complex permittivity (Cont'd)			

DD FORM 1 JAN 73 1473

157000

gum

UNCLASSIFIED

SECURITY CLASSIFICATION OF THIS PAGE (When Data Entered)

79 06 08 008

Item 20 (Cont'd)

of the ground ranged from $5 + 10.6$ to $14 + 12.0$ or $k_g/k_o = 2.2 + 10.1$ to $3.8 + 10.3$, respectively.

A theoretical treatment of the scattering from horizontal-wire antennas over the earth is presented in Part II. The well-known electromagnetic fields generated by infinitesimal dipoles in the presence of the earth are reviewed briefly. The fields due to currents in extended conductors can be expressed in terms of an integral over the occupied volume, but its evaluation is possible only when the currents are known in their dependence on the properties of the earth. This is true of the horizontal-wire antenna quite close to the earth, both when driven by a localized emf and when acting as a scatterer in an incident field. Expressions for the most useful component of the radiated or scattered field are formulated for an end-driven Beverage-type antenna and the horizontal-wire as a scatterer in the presence of the earth.

Accession For	
NTIS GML&I	<input checked="" type="checkbox"/>
DDC TAB	<input type="checkbox"/>
Unannounced	
Justification	
By _____	
Distribution/	
Availability	
Dist.	Available or special
A	

UNCLASSIFIED

SUMMARY

The discovery and identification of a vehicle or other obstacle on or above the earth by radar from the air is difficult because the reflected signal from the obstacle is obscured by the signals scattered from the earth. The intensity of these latter depends on the reflecting and absorbing properties of the earth's surface, which may be dry, moist, or frozen soil; lake or sea water; or ice or snow — all with very different electrical characteristics. Furthermore, the angle of the incident beam can range from nearly grazing to perpendicular to the earth's surface. Depending on the proximity of the obstacle to the earth, the currents induced in it which generate the reflected field may differ significantly from their values in the absence of the earth with corresponding changes in the reflected field and in the identifiable characteristics of the obstacle.

The primary objective of the task is to determine the effect of the earth on signals scattered from simple obstacles — especially circular loops and combinations of loops as well as dipoles — in its relation to the properties and the proximity of the earth's surface.

The technical problem involves the following: 1) A theoretical and experimental study of the currents induced in circular loops with various sizes when isolated and when at different heights over the earth. The loops are illuminated by a plane wave arriving with different angles of incidence. 2) The determination of the scattered field due to the induced currents as compared with the fields due to the currents in the loops in the absence of the earth. The methods used include the solution of Maxwell's equation subject to appropriate boundary conditions and the direct measurement with a suitably designed experiment. This includes measurements on loops over soil at an outdoor site and measurements over a tank of water indoors. An apparatus has been constructed at an outdoor site and measurements have been completed on single circular loops and dipoles over the earth. These indicate substantial effects due to the earth over a range of heights up to one wavelength. The indoor apparatus for measurements over water has been completed and tested and measurements are in progress.

A rigorous theoretical formulation has been completed. This involves the so-called Sommerfeld integrals. A new method of solution using the

variational principle is being developed. It is hoped to compare theoretical and experimental results when both are available.

When the solution of the problem of scattering from the single circular loop at an arbitrary distance over the earth has been completed and verified experimentally, two and more coaxially placed loops will be investigated as a first approach to a three-dimensional vehicle.

TABLE OF CONTENTS

PAGE

**PART I: Measurement of the Scattered Fields from a Metal Loop
and a Straight Wire Placed Above the Ground**

1.1. Introduction. 1

1.2. Experimental Setup. 1

1.3. Transmitting and Receiving Antennas 5

1.4. Properties of the Ground. 5

1.5. The Scatterers. 8

1.6. Experimental Results. 8

1.7. Experimental Setup to Measure the Back Scattered
Field from Conductive Loops Above Water 11

PART II: Theory of Scattering from Horizontal-Wire Antennas

2.1. Introduction. 31

2.2. Currents and Field of the Driven Horizontal-Wire
Antenna Over the Earth. 31

2.3. Scattering by the Horizontal-Wire Antenna
Over the Earth. 38

2.4. Conclusion. 44

REFERENCES. 45

PART I
MEASUREMENT OF THE SCATTERED FIELDS FROM A METAL LOOP AND A STRAIGHT WIRE
PLACED ABOVE THE GROUND

1.1. Introduction

A knowledge of the scattered field from objects located above a dielectric half-space is of interest in radar. While the well-known Sommerfeld problem of radiation from a Hertzian dipole in such an environment has received extensive study in the past (see bibliographies in [1]-[3]), the determination of the surface current distribution induced on a finite object by an incident plane wave remains unsolved. This surface density of current, which corresponds to a continuous distribution of infinitesimal dipoles that are dependent on the geometrical and electrical properties of the scattering object and the presence of the dielectric half-space, must be evaluated before the solution of the Sommerfeld problem can be applied to find the scattered field.

A conducting thin circular loop is chosen as the scatterer because of its geometrical simplicity, because a solution for the current in the loop can be extended readily to cylindrical or other objects, and because when it is in free space, the current distribution is known [4]. Experiments are being carried out to measure the scattered field from loops of different sizes at different heights above earth and water.

1.2. Experimental Setup

The frequency used in this experiment was set at 1.5 GHz, which corresponds to a free-space wavelength of 20 cm. The transmitting antenna was supported by a quarter-circular arc, as shown in Fig. 1. The structure was made of low-density polyfoam with dielectric constant approximately equal to 1.02. Radial holes were drilled every 15 degrees in the arc so that the transmitting antenna could be mounted at different positions in order to launch waves with various angles of incidence. The transmitting antenna was 2 m or 10 wavelengths away from the scatterer. The latter was sufficiently far from the antenna so that it could be considered to be illuminated by a uniform plane wave.

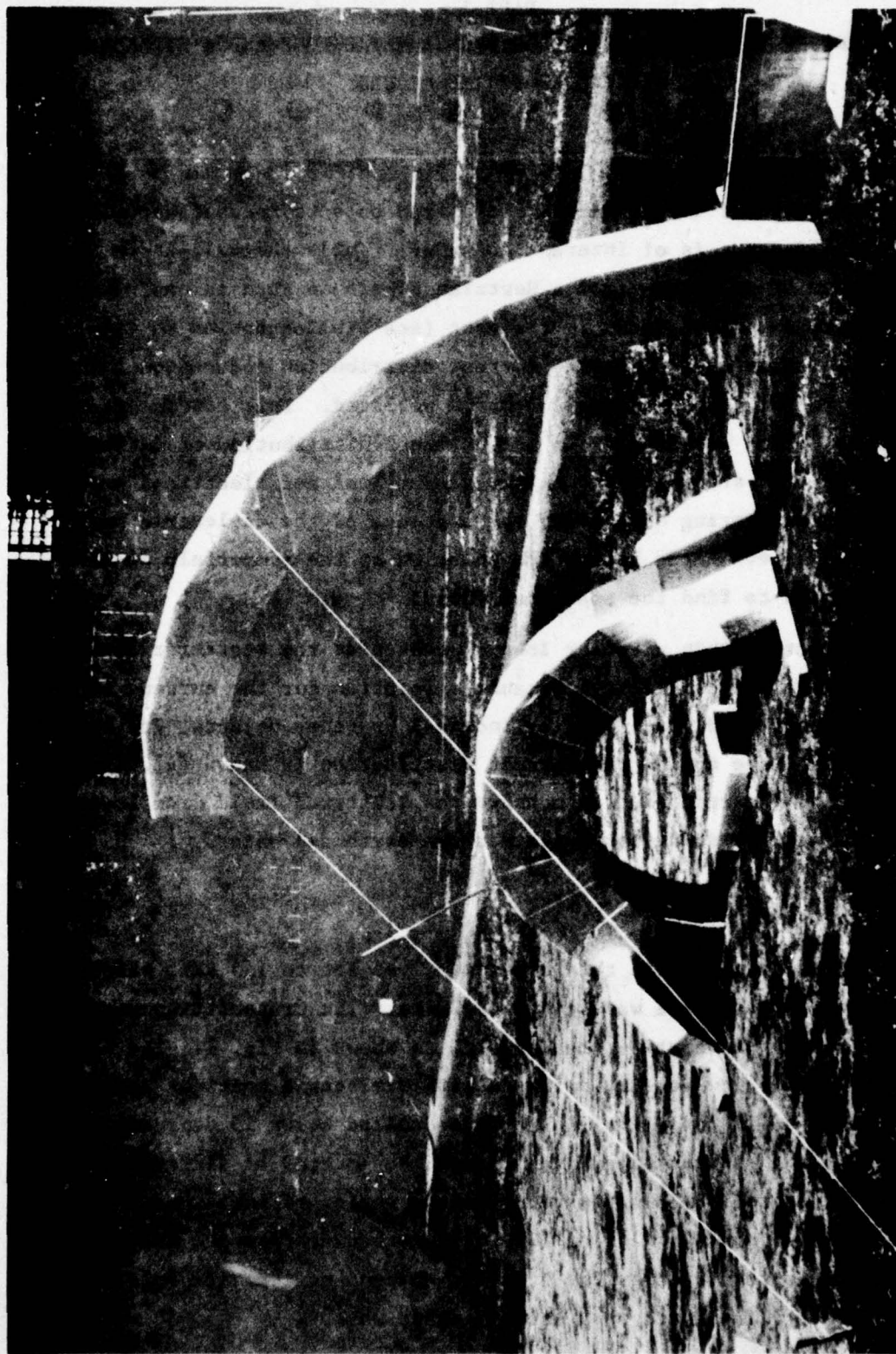


Fig. 1. Photograph of the polyfoam support structures for the transmitting and receiving antennas.

The structure that supported the receiving antenna was a semi-circular arc made of polyfoam, as shown in Fig. 1. The receiving antenna was fixed on a plexiglass rod which could be inserted into one of the radial holes drilled every 15 degrees on the polyfoam arc. The distance between the receiving antenna and the scatterer was 1.5 m or 7.5 wavelengths. The semi-circular polyfoam arc could be rotated to vary the azimuthal angle of the receiving antenna. The azimuthal angle was marked by wooden golf tees embedded every 10 degrees in the ground on a circle of 1 meter radius. To check the effect of the polyfoam and the layers of glue in the semi-circular arc, the signal from the transmitting antenna was measured by the receiving antenna with the polyfoam arc placed at various positions and angles between the two. No difference in amplitude of the received signal could be detected, and the change in phase of the received signal varied less than 3 degrees. It was concluded that the structure did not change the incident wave or the scattered wave in any significant manner.

The block diagram of the experimental setup is shown in Fig. 2. The key element in the setup was the hybrid, which made possible the complete cancellation of the incident and reflected fields and the field from the transmitting antenna picked up directly by the receiving antenna. The procedure was as follows. With the transmitting antenna and the receiving antennas set in their respective positions, the scatterer or target was removed and the variable attenuator and phase shifter were adjusted to obtain a null reading on the vector voltmeter. The scatterer was then put into position. The reading on the voltmeter was recorded as the scattered field strength. It was found during the experiment that the direct pick-up by the receiving antenna in the absence of the scatterer was approximately 30 dB higher than the scattered field. It would have been impossible to detect any change in reading with and without the scatterer present if this cancellation scheme had not been used. The null or noise level which the cancellation circuit was able to achieve was found to be better than -40 dB below the uncanceled signal, thus giving a range of about 10 dB for detection of the scattered field strength which, as mentioned earlier, was about -30 dB below the uncanceled signal.

The structure that supported the receiving antenna was a semi-circular arc made of polyethylene, as shown in Fig. 1. The receiving antenna was fixed on a horizontal rod which could be translated into one of the radial rails drilled every 12 degrees in the polyethylene. The distance between the receiving antenna and the scatterer was 1.5 m or 1.7 waves longer. The exact distance between the scatterer and the receiving antenna was varied by means of the receiving antenna. The scattered signal was picked up by a horn antenna which was 15 degrees in diameter and was fixed on a frame of 1 meter radius. To check the effect of the scatterer on the signal, the horn antenna was moved in the semi-circular arc, the signal was measured by the receiving antenna and the distance between the scatterer and the receiving antenna was varied by the receiving antenna. The distance between the scatterer and the receiving antenna was varied by the receiving antenna. The distance between the scatterer and the receiving antenna was varied by the receiving antenna.

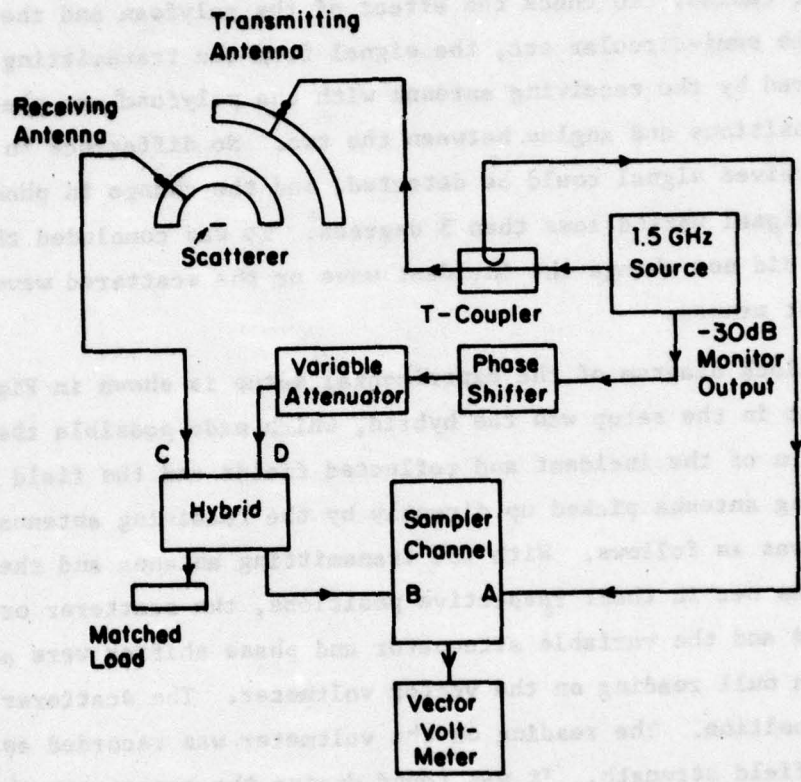


Fig. 2 Block diagram of experimental setup

1.3. Transmitting and Receiving Antennas

The transmitting antenna used in this experiment was a half-wave, folded dipole with one parasitic element, 0.51 wavelength in length and spaced 0.25 wavelength behind the folded dipole, which acted as a reflector. The signal was fed through a section of coaxial line, a balun, and a 10-meter long shielded two-wire line before it reached the folded dipole. The balun was adjusted until the most symmetrical field pattern was obtained. The field pattern is shown in Fig. 3a. The receiving antenna was similarly constructed, except that the shielded two-wire line was 7 meters long. The balanced field pattern for the receiving antenna is shown in Fig. 3b. It should be noted that, although these antennas had neither high gains nor narrow beams, the cancellation scheme described in the previous section eliminated the need for longer or more complex arrays. Furthermore, balancing the two-wire line using a simple balun at 1.5 GHz for a long array was found to be rather difficult to accomplish.

In order to minimize interference with the incident and received fields, the wires attached to both antennas were supported by wooden stands and were either perpendicular to the polarization of the wave, or lying on and shielded by the ground. The polarization of both the incident and received waves was in the ϕ -direction (azimuthal direction). The supporting structure for the antenna contributed to a depolarized component of -14 dB in the forward direction. This level of polarization purity was considered to be adequate.

1.4. Properties of the Ground

The ground over which the scatterer was placed was soil with no vegetation within one meter of the scatterer. There were no utility cables or pipes under the experimental area, except for a plastic sewer pipe, 15 cm in diameter, approximately 2 meters below the surface. The skin depth of the soil at 1.5 GHz was less than 20 cm. Thus the presence of the pipe could not have affected the measurements.

The complex permittivity of the soil sample on the ground of the experiment was measured with various moisture contents and at different depths. A General Radio 10 cm, coaxial air-line was modified to hold a

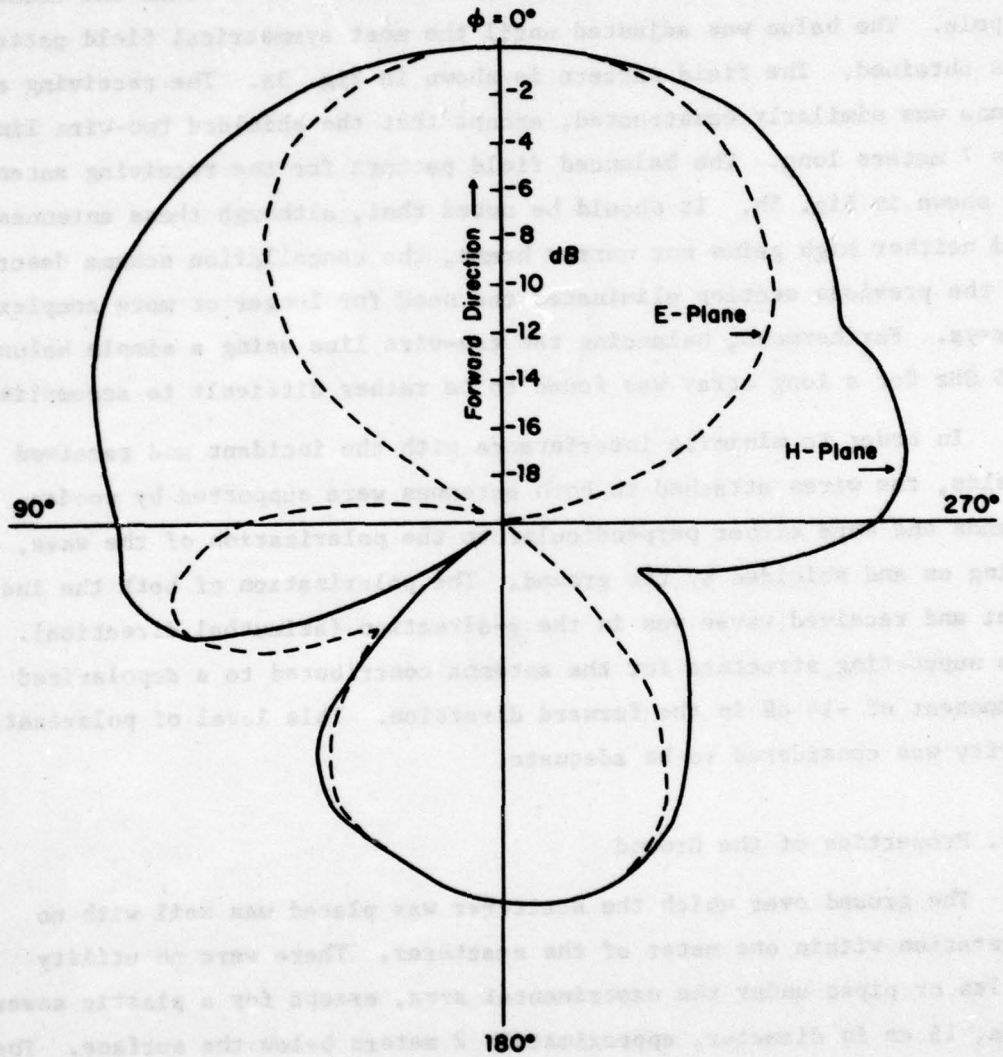


Fig. 3a Balanced field pattern for transmitting antenna

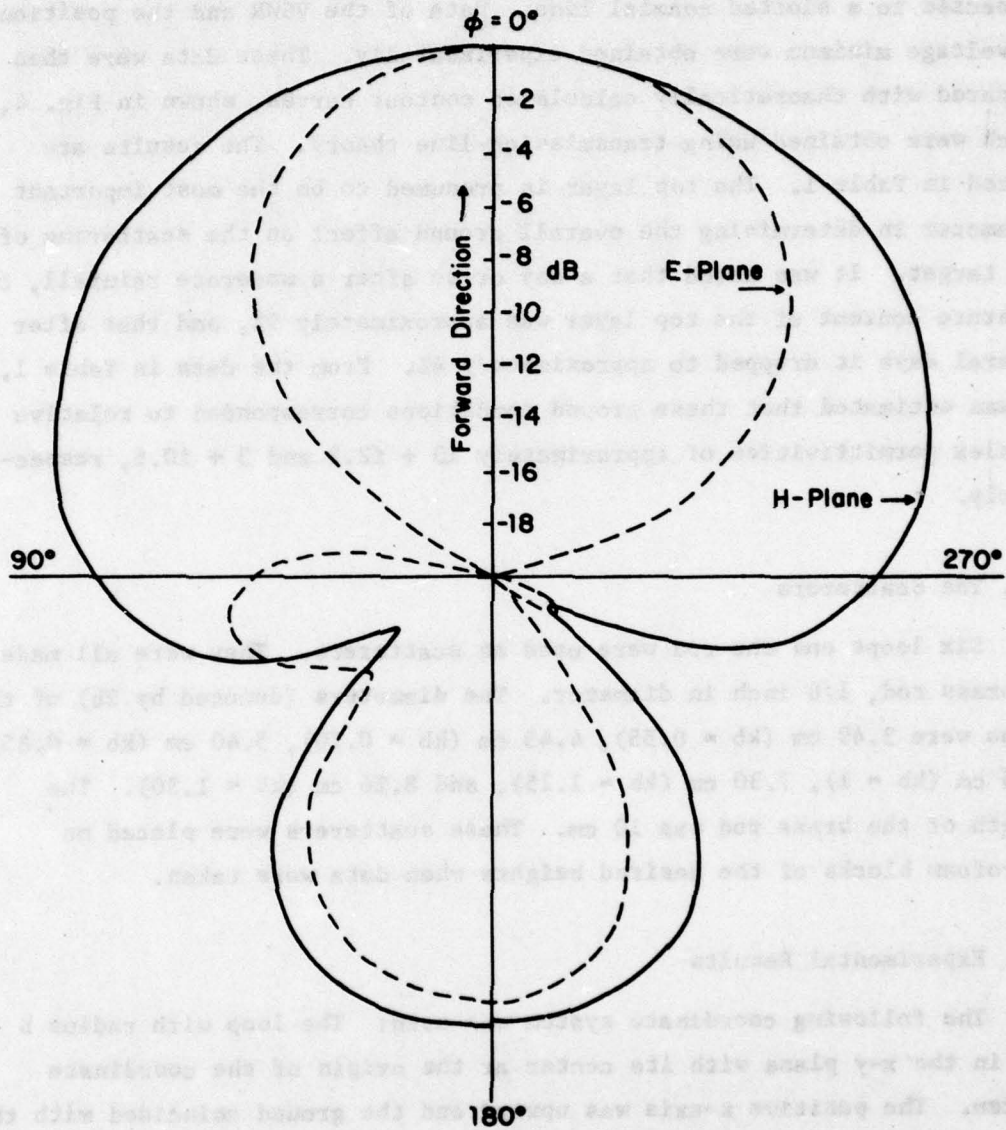


Fig. 3b Balanced field pattern for receiving antenna

sample 2 cm in length, with a 1.9 cm section of the remaining line filled with air, and then short-circuited at the end. This sample holder was connected to a slotted coaxial line. Data of the VSWR and the position of voltage minimum were obtained experimentally. These data were then compared with theoretically calculated contour curves, shown in Fig. 4, which were obtained using transmission-line theory. The results are listed in Table 1. The top layer is presumed to be the most important parameter in determining the overall ground effect on the scattering of the target. It was noted that a day or so after a moderate rainfall, the moisture content of the top layer was approximately 9%, and that after several days it dropped to approximately 4%. From the data in Table 1, it was estimated that these ground conditions corresponded to relative complex permittivities of approximately $13 + j12.2$ and $5 + j10.6$, respectively.

1.5. The Scatterers

Six loops and one rod were used as scatterers. They were all made of brass rod, 1/8 inch in diameter. The diameters (denoted by $2b$) of the loops were 3.49 cm ($kb = 0.55$), 4.45 cm ($kb = 0.70$), 5.40 cm ($kb = 0.85$), 6.35 cm ($kb = 1$), 7.30 cm ($kb = 1.15$), and 8.26 cm ($kb = 1.30$). The length of the brass rod was 10 cm. These scatterers were placed on styrofoam blocks of the desired heights when data were taken.

1.6. Experimental Results

The following coordinate system was used: The loop with radius b lay in the x - y plane with its center at the origin of the coordinate system. The positive z -axis was upward and the ground coincided with the $z = -h$ plane. The axis of the transmitting antenna lay in the x - z plane with its dipole pointing to the y -direction. The incident wave traveled in the positive x and negative z directions.

The location of the transmitting antenna was described in spherical coordinates by $r = 2.15$ m, the polar angle θ_t , and the azimuthal angle $\phi_t = 180^\circ$, while that of the receiving antenna was denoted by $r = 1.5$ m, and θ_r , ϕ_r .

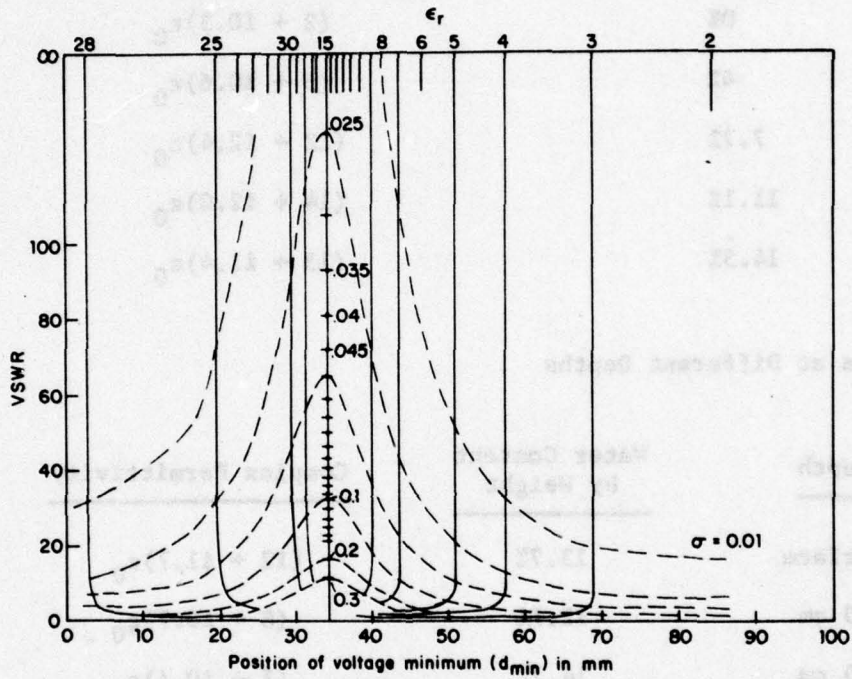


Fig. 4 Theoretical curves of conductivity σ and relative permittivity ϵ_r for 2cm soil sample in coaxial line, $f = 1.5$ GHz.

TABLE 1
MEASURED RELATIVE COMPLEX PERMITTIVITY

(a) Sample at Surface Layer

<u>Water Content by Weight</u>	<u>Complex Permittivity</u>
0%	$(2 + 10.3)\epsilon_0$
4%	$(5 + 10.6)\epsilon_0$
7.7%	$(12 + 12.4)\epsilon_0$
11.1%	$(14 + 12.0)\epsilon_0$
14.3%	$(15 + 11.4)\epsilon_0$

(b) Sample at Different Depths

<u>Depth</u>	<u>Water Content by Weight</u>	<u>Complex Permittivity</u>
Surface	13.7%	$(12 + 11.7)\epsilon_0$
10 cm	12.7%	$(8 + 10.7)\epsilon_0$
20 cm	14.2%	$(7 + 10.4)\epsilon_0$
30 cm	13.3%	$(6 + 10.4)\epsilon_0$

The scattered power is given in Figs. 5a-c as a function of ϕ_r , in Figs. 6a,b as a function of θ_r , in Figs. 7a,b as a function of the size of the loop, and in Figs. 8a-d as a function of the height of the loop above the earth.

The measurements were restricted to horizontal polarization of the electric field with the loop placed horizontally above the earth. Even with this restriction, the measurement of the complete scattered field of loops of different sizes, at different heights, and with fields incident at different angles, was a forbidding task. Since the variation of the parameters associated with the loop was of fundamental importance in checking a correct theory, it was decided to reduce the data in future measurements by obtaining only the back scattered fields which are of primary practical importance.

When carrying out the cancellation technique suggested by T. T. Wu, it was possible to obtain a noise background as low as -65 dBm. But when the scattered signal was -55 dBm or below, when the loop was small (Figs. 7a,b), or when the loop was at particular heights (Fig. 8d), it was not possible to obtain an accurate reading or, in some cases, to detect any signal at all. While the meter can read up to 10 dBm and the strongest signal obtained was around -37 dBm - assuming that a noise background at the level of -65 dBm can always be achieved - it is desirable to increase the power output of the transmitting antenna for the next experiments.

1.7. Experimental Setup to Measure the Back Scattered Field from Conductive Loops Above Water

a) Operating frequency. 1.5 GHz was chosen to be the working frequency. The dielectric constant for pure water at this frequency was estimated to be $77\epsilon_0(1 + i0.0785)$.

b) The scatterer. Seven loops made of brass strips, 3 mm wide and 0.0762 mm thick, were used as scatterers. The circumference of the loops increased from 11 cm to 29 cm in 3 cm steps.

c) The transmitting antenna. A six-element Yagi array was used as the transmitting antenna. According to calculations by King *et al.* [5],

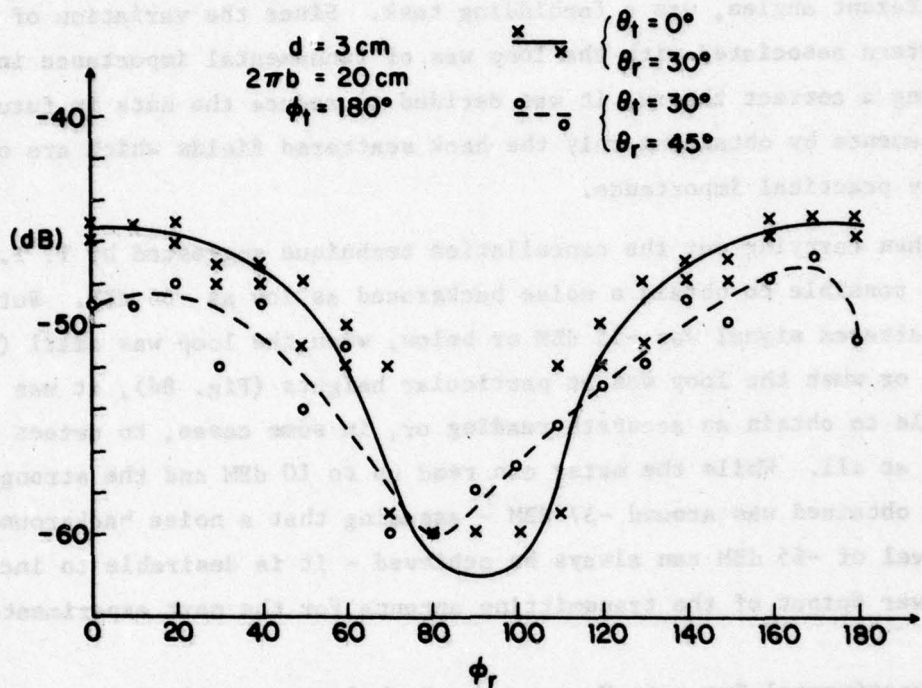


Fig. 5a Measured $|E^2|$ scattered from loop at a height d over the earth ($\tilde{\epsilon}_r = 5 + i0.6$) as a function of ϕ_r .

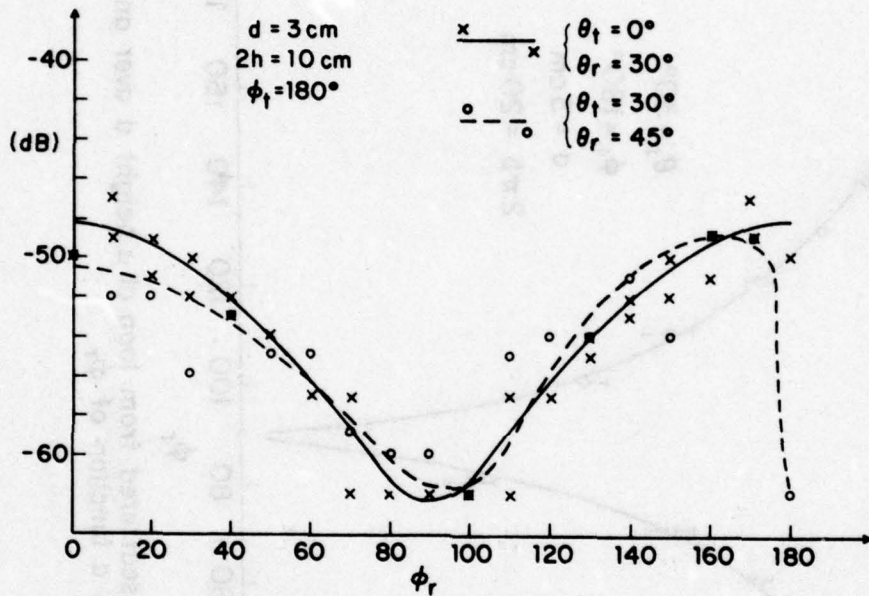


Fig. 5b Measured $|E^2|$ scattered from brass rod at a height d over the earth ($\epsilon_r \approx 5 + i0.6$) as a function of ϕ_r .

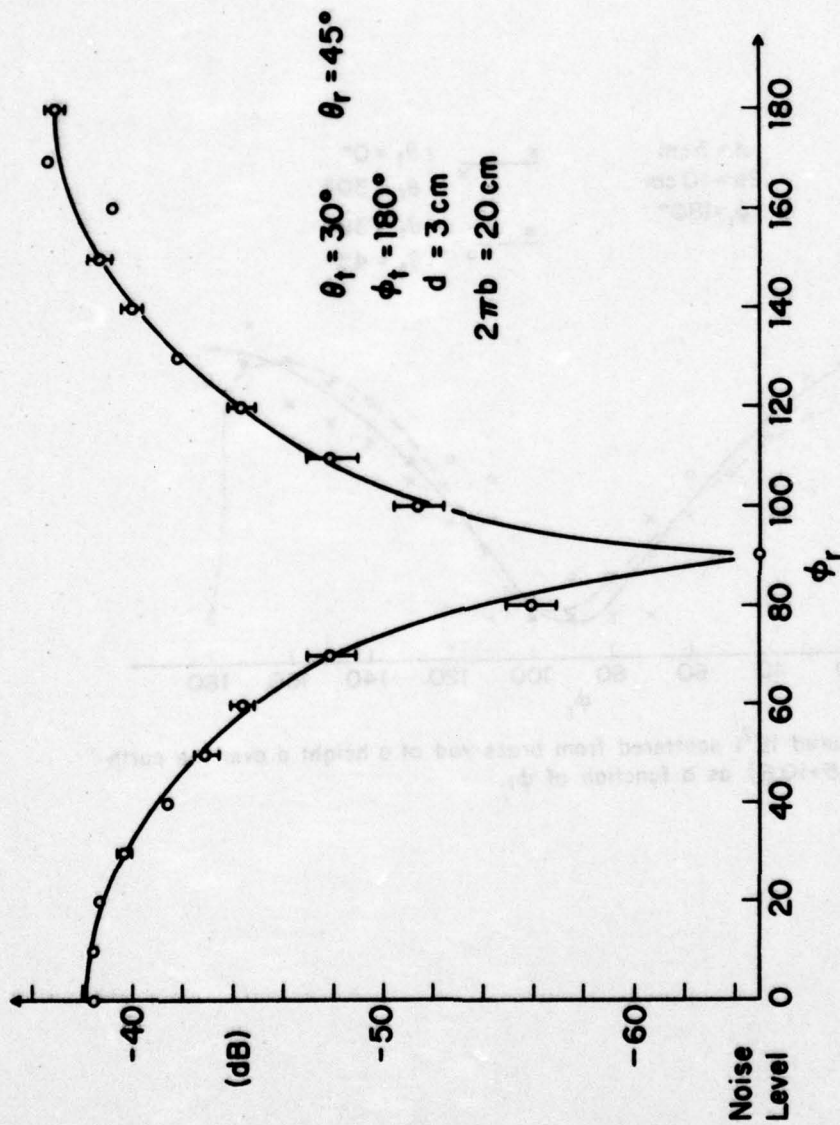


Fig. 5c Measured $|E^2|$ scattered from loop at a height d over an aluminum ground plane as a function of ϕ_r

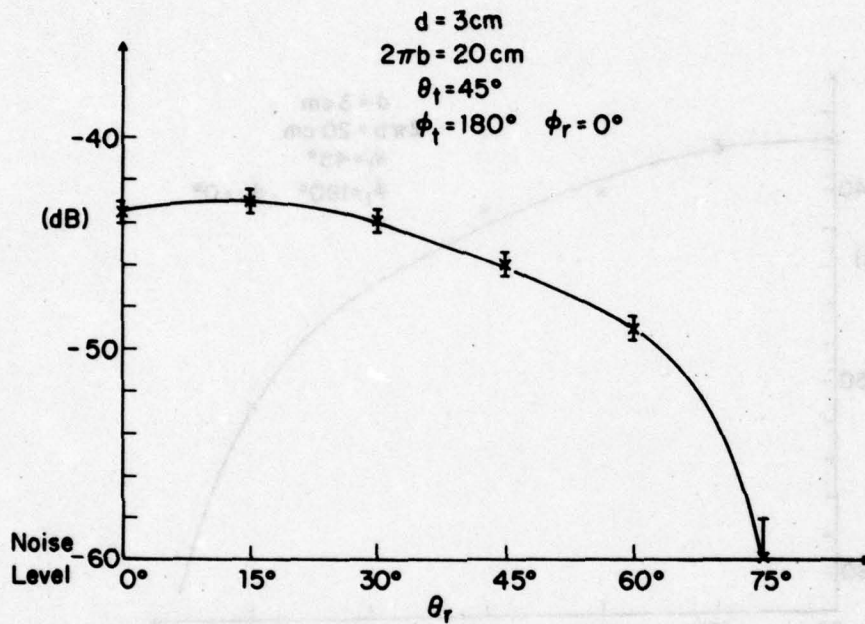


Fig. 6a Measured $|E^2|$ scattered from loop at a height d over the earth ($\tilde{\epsilon}_r = 14 + i2.0$) as a function of θ_r .

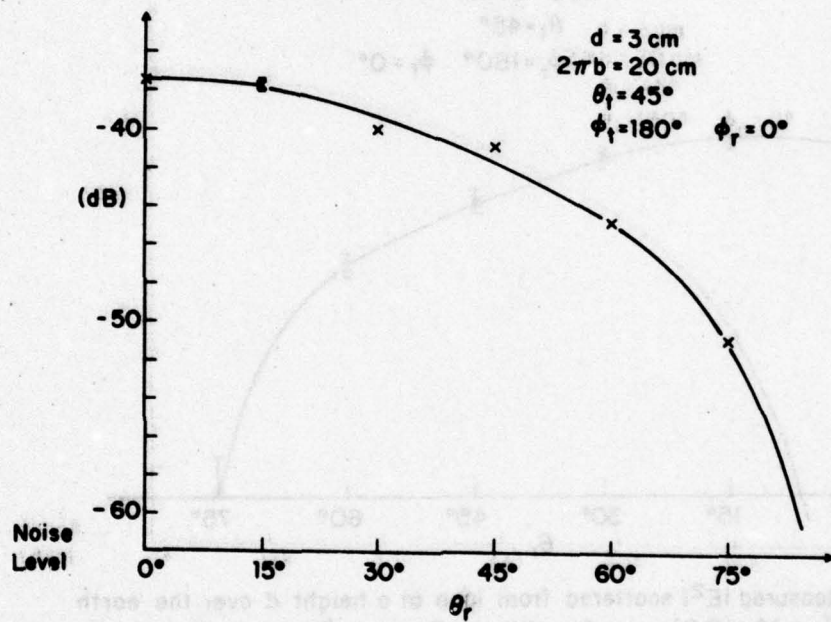


Fig. 6b Measured $|E^2|$ scattered from loop at a height d over an aluminum ground plane as a function of θ_r .

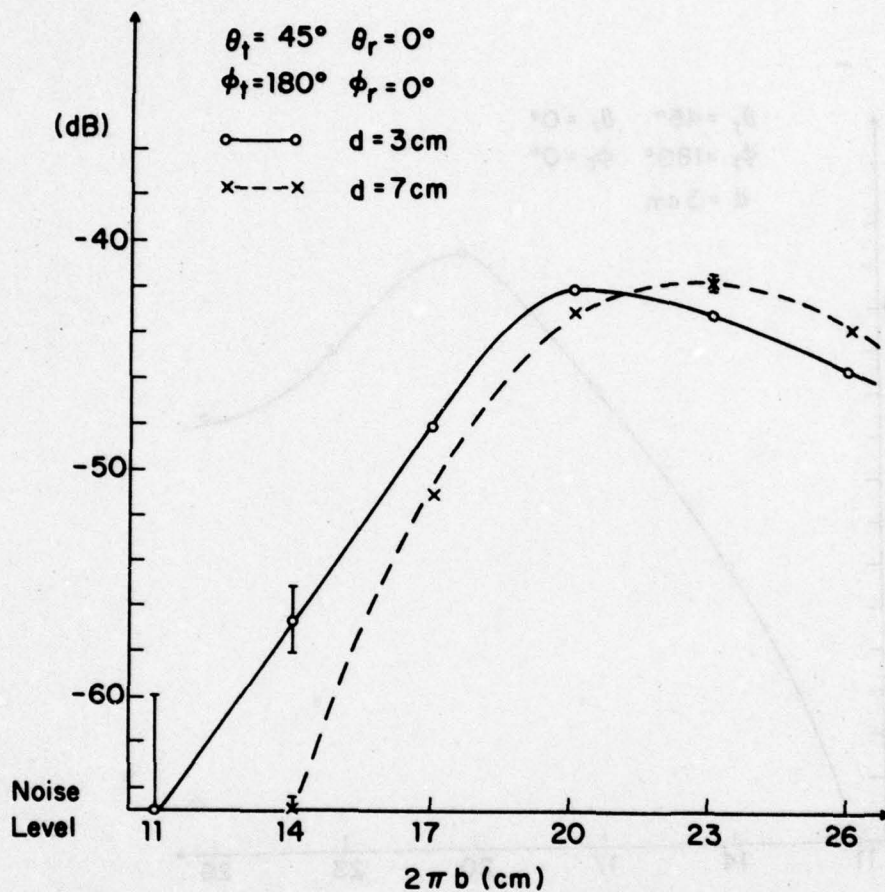


Fig. 7a Measured $|E^2|$ scattered from loop at a height d over the earth ($\epsilon_r \approx 14 + i2.0$) as a function of the size of the loop.

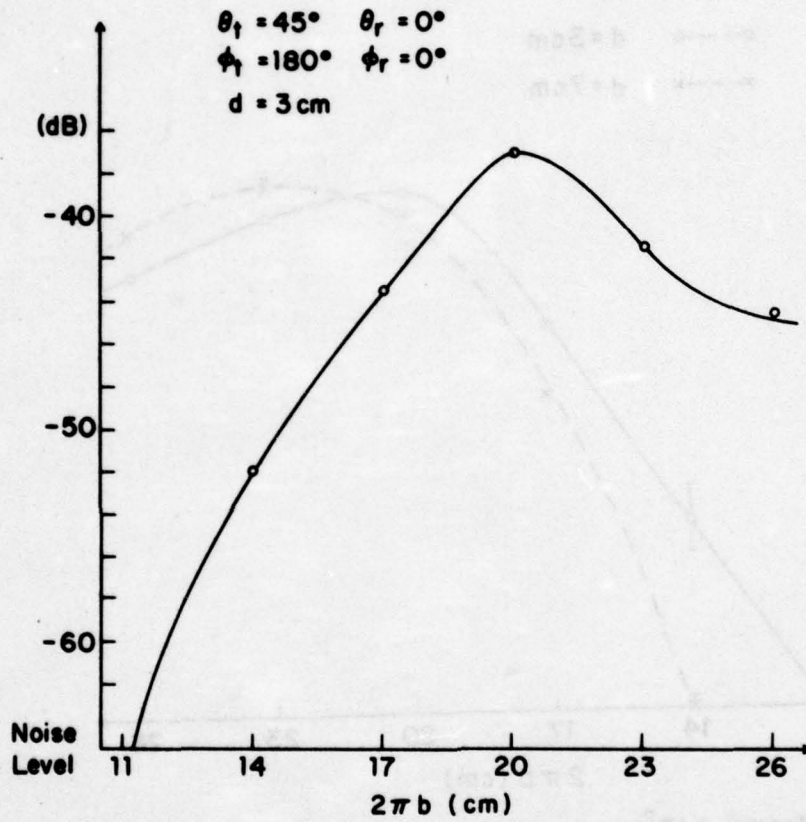


Fig. 7b. Measured $|E^2|$ scattered from loop at a height d over an aluminum ground plane as a function of the size of the loop.

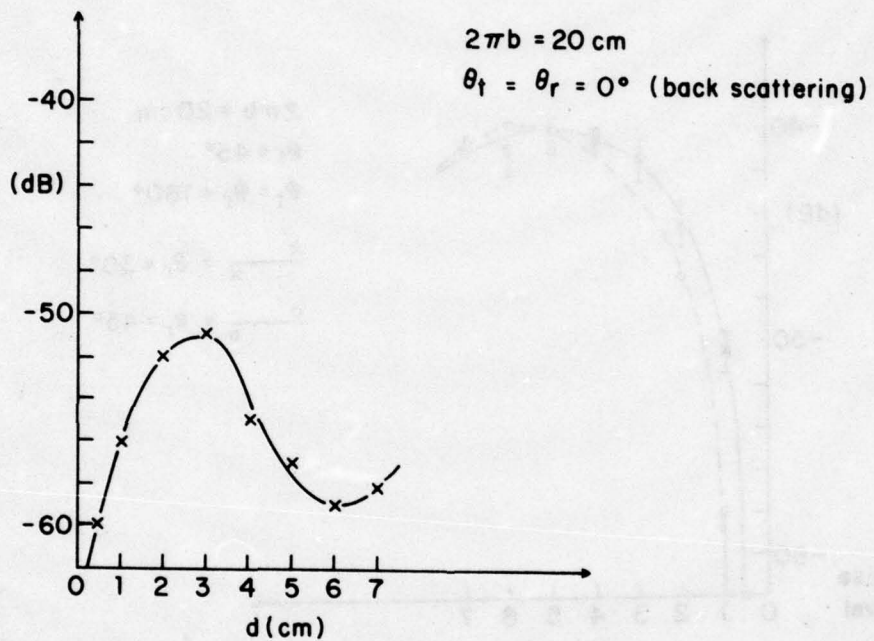


Fig. 8a Measured $|E^2|$ scattered from loop as a function of its height d over the earth ($\tilde{\epsilon}_r = 5+i0.6$).

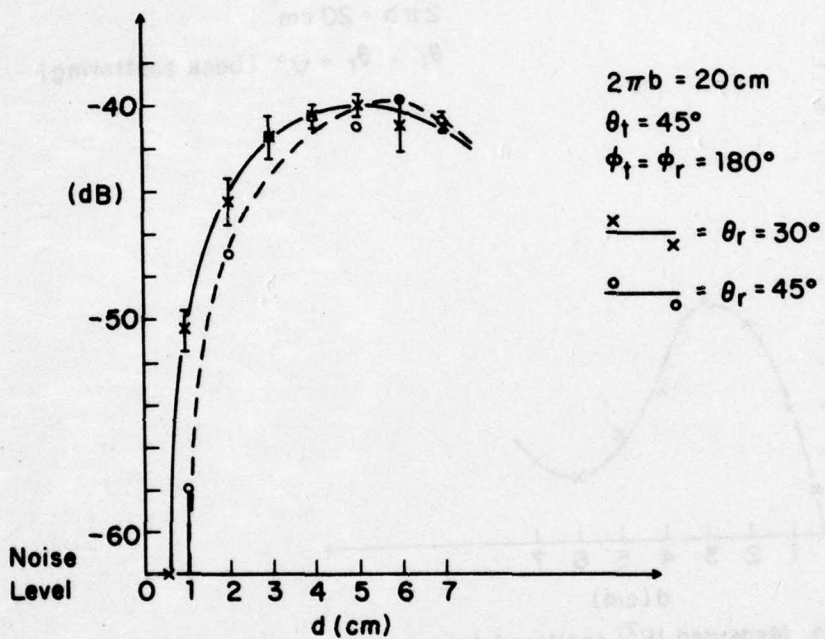


Fig. 8b Measured $|E^2|$ scattered from loop as a function of its height d over the earth ($\epsilon_r \approx 14+i2.0$).

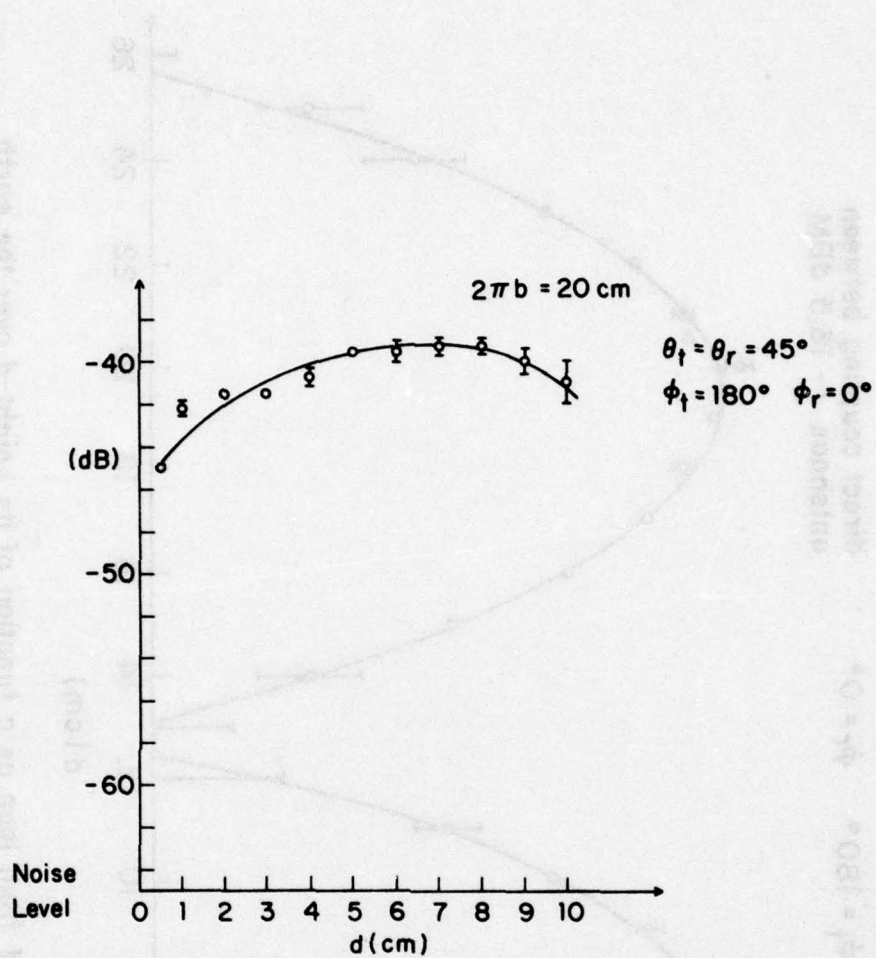


Fig. 8c Measured $|E^2|$ scattered from loop as a function of its height d over an aluminum ground plane.

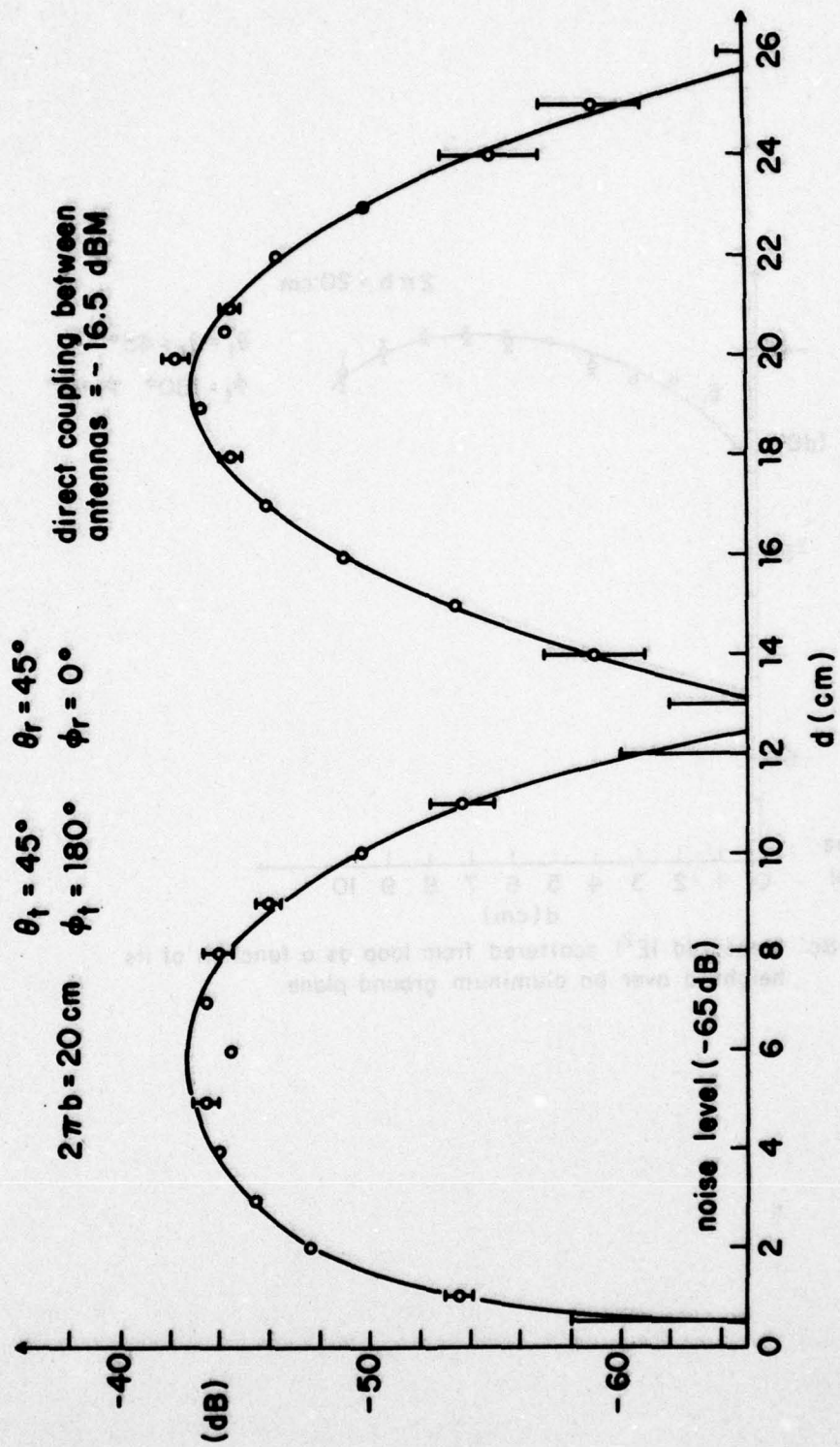


Fig. 8d Measured $|E^2|$ scattered from loop as a function of its height d over the earth
 $(\bar{\epsilon}_r = 14 + i2.0)$.

a maximum front-to-back ratio could be obtained if the four directors and the driven element were 8.52 cm long and equally spaced at 4.96 cm intervals, and the reflector were 10.2 cm in length and 5 cm away from the driven element. Because the four directors were supported by an acrylic bar 0.5 inch in diameter, the length of the directors had to be adjusted to achieve optimal forward gain. By trial and error, a length of 8.02 cm was selected for the directors. The field pattern in the plane containing the axis and the directors of the antenna is shown in Fig. 9a. A back-to-front ratio of -22 dB was obtained and all the side lobes were -19 dB below the main one.

The elements of the Yagi array were made of 1/8 inch diameter brass rods. It was driven by two rods of the same diameter, separated by 1/16 inch to form a two-wire line. These two wires were held in position by the same 1/2 inch diameter acrylic bar that supported the directors and the driven element. This two-wire section, which was 20 cm long, was inserted into a brass tube 45 cm long with a half inch inner diameter so as to form a section of shielded two-wire line with an impedance of about 65 ohms. This was designed to match approximately the input impedance of the Yagi array which had a resistive part of about 62 ohms [5].

The two-wire line section was connected to a 25 cm long coaxial-line section inside the same shielding brass tube. Two slots were cut in the shielding tube in the plane bisecting the elements of the Yagi array. A double ring, one part filling the space between the exterior of the coaxial line and the inside wall of the shielding tube, the other part enclosing the shielding tube, was screwed together through the slots to form a convenient sleeve-type adjustable single-frequency balun. Two sets of springy brass fingers were attached to the inner ring to assure good contact with both tubes. Without them, the balun did not work at all. The balun was then connected to an N-type bulkhead receptacle to be connected to the power source.

d) The receiving antenna. A folded dipole with a reflecting element comprised the receiving antenna. A shielded two-wire line led the signal from the folded dipole to a modified GR 874-UB balun. The balun was extended in length by inserting four connectors into it so that it could be tuned to work at 1.5 GHz. The field pattern in the plane containing the

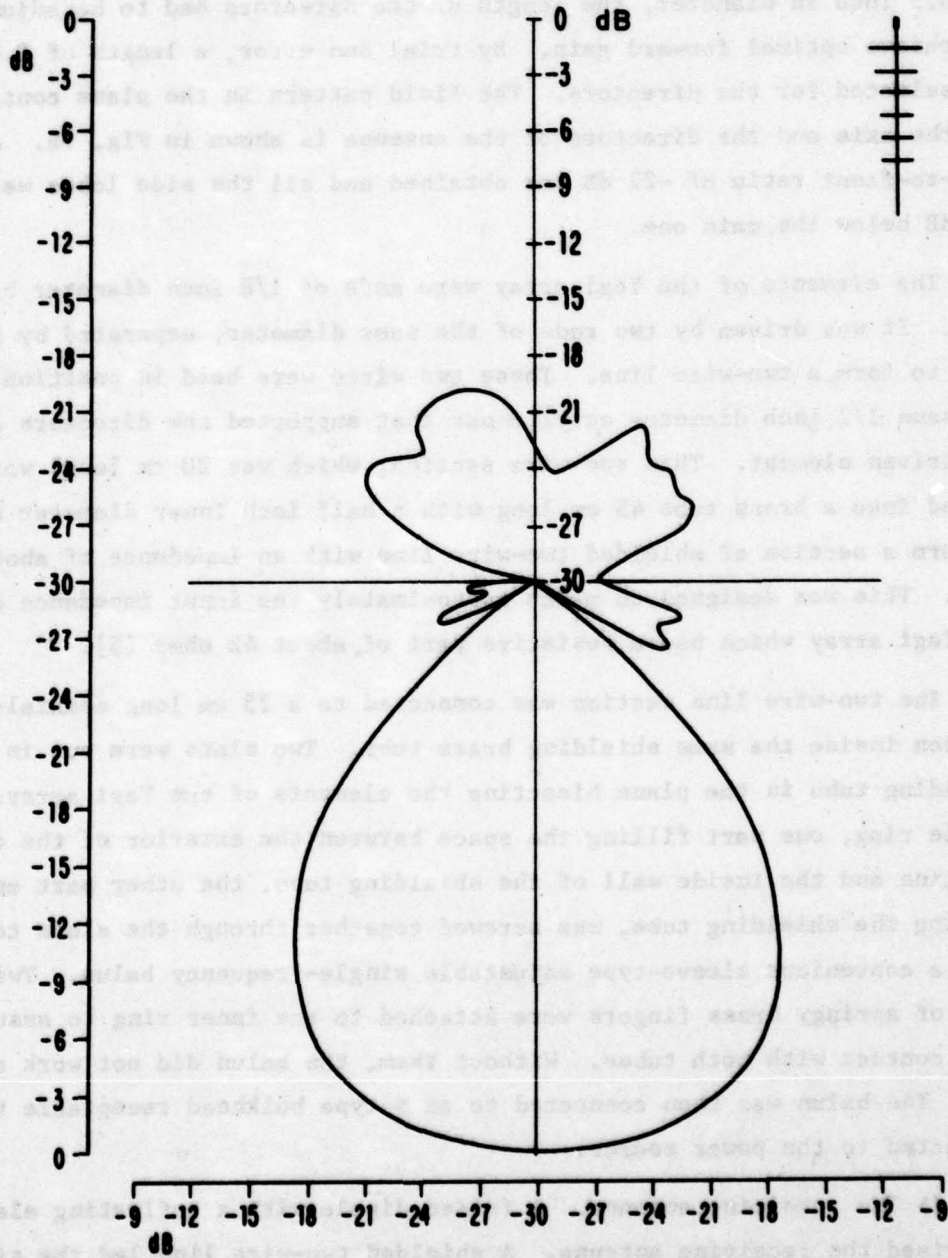


Fig. 9a Field pattern in plane of four-director Yagi antenna.

antenna axis and the driven element is shown in Fig. 9b.

The receiving antenna was attached to the transmitting antenna with the driven and reflecting elements facing and parallel to one another to obtain the back scattered field. The front-to-back ratio of the receiving antenna was enhanced by the presence of the directors of the transmitting antenna.

The antennas were then put into a cubic box consisting of one layer of Ecosorb H-4 sandwiched between styrofoam blocks that enclosed the sides and backward direction of the antennas and left an opening that extended through an angle of $57^{\circ}.4$ from the driving point. The resulting far field patterns of the transmitting and receiving antennas are shown in Figs. 10a,b for the planes containing the respective axes and the driven element, and in Figs. 10c,d for the plane bisecting the driven element.

e) Supporting structure. A wooden octagonal water tank was built which was 303 cm in diagonal dimension and 61 cm deep. A Sears vinyl liner for swimming pools, 10 feet in diameter and 2 feet deep, was used to prevent water leakage. The seam and drainage plug of the liner were taped using a vinyl repair kit in order further to achieve this goal.

A styrofoam semi-circular arch, 400 cm in inner diameter, was built to support the antennas. The entire arch could be raised upward in 1 cm steps with 0.3175 cm and 0.635 cm as intermediate heights. The antenna set was mounted on the arch for incident angles of 45° and a range from 0° to 80° in 10° increments.

A 50 cm square, 5 cm thick, plate of styrofoam was hung from the top of the semi-circular supporting arch by four vertical Trilene Monofilament fish lines. A 40 cm diameter disc was drilled in the center of this plate. Seven similar discs were made, each with a loop embedded from below. This allowed the loop to be lowered as close to the water surface as desired. Since the center of the loop coincides with the center of the semi-circular supporting arch and the antenna set always moves with this structure, the antennas are always pointing to the center of the loop.

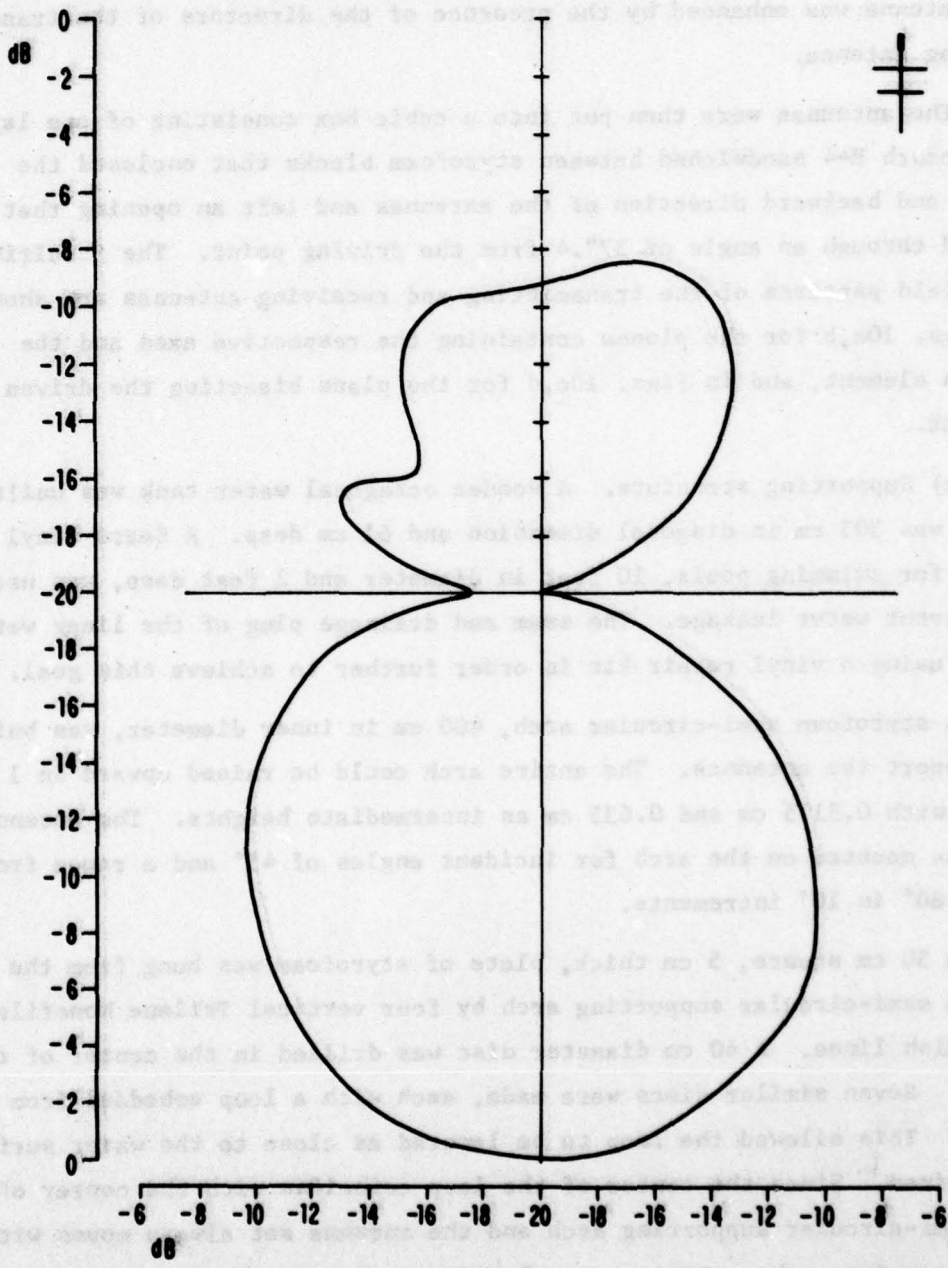


Fig. 9b Field pattern in plane of folded dipole with reflector

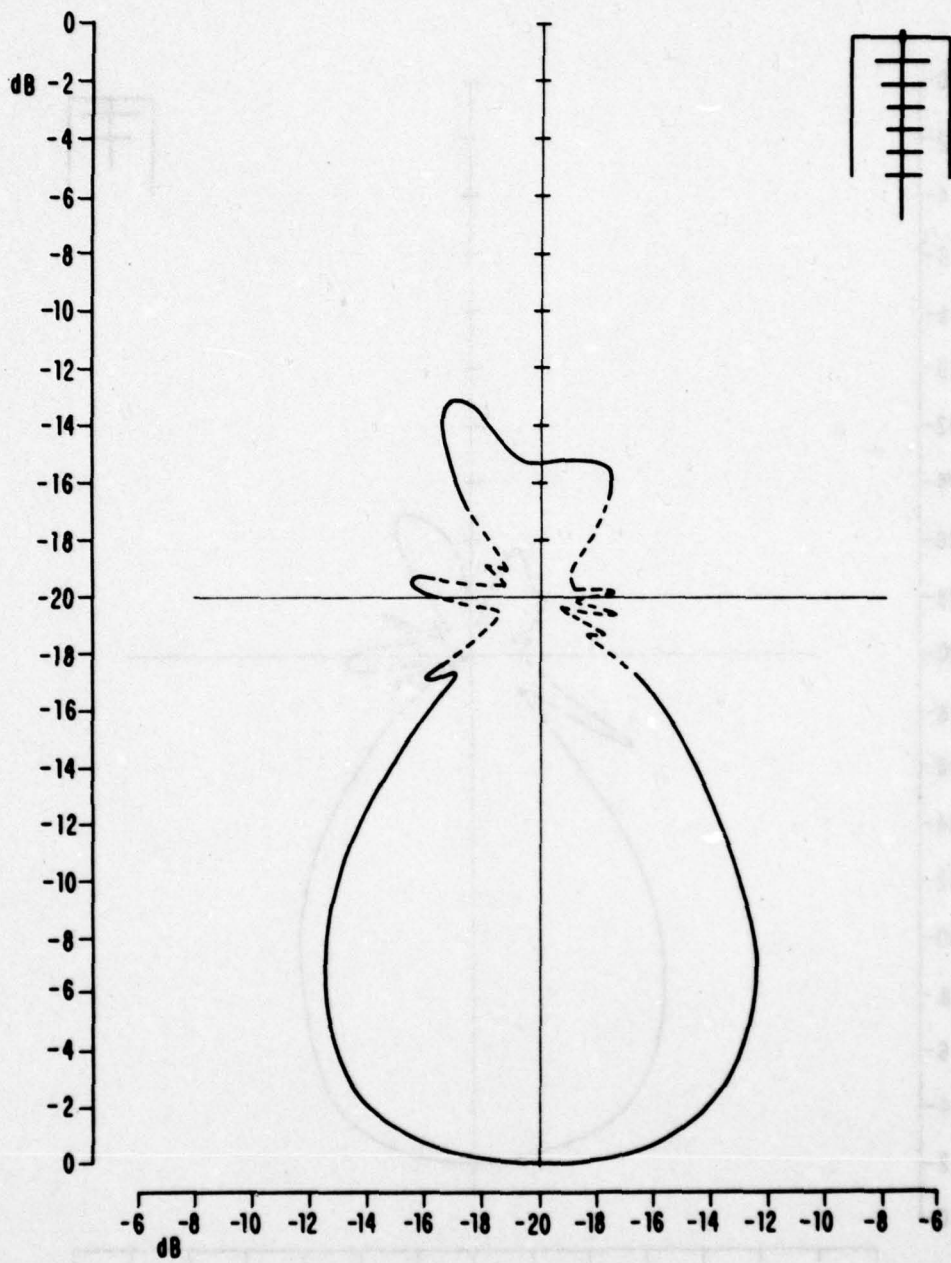


Fig. 10a Field pattern in plane of elements of transmitting Yagi with absorbing walls.

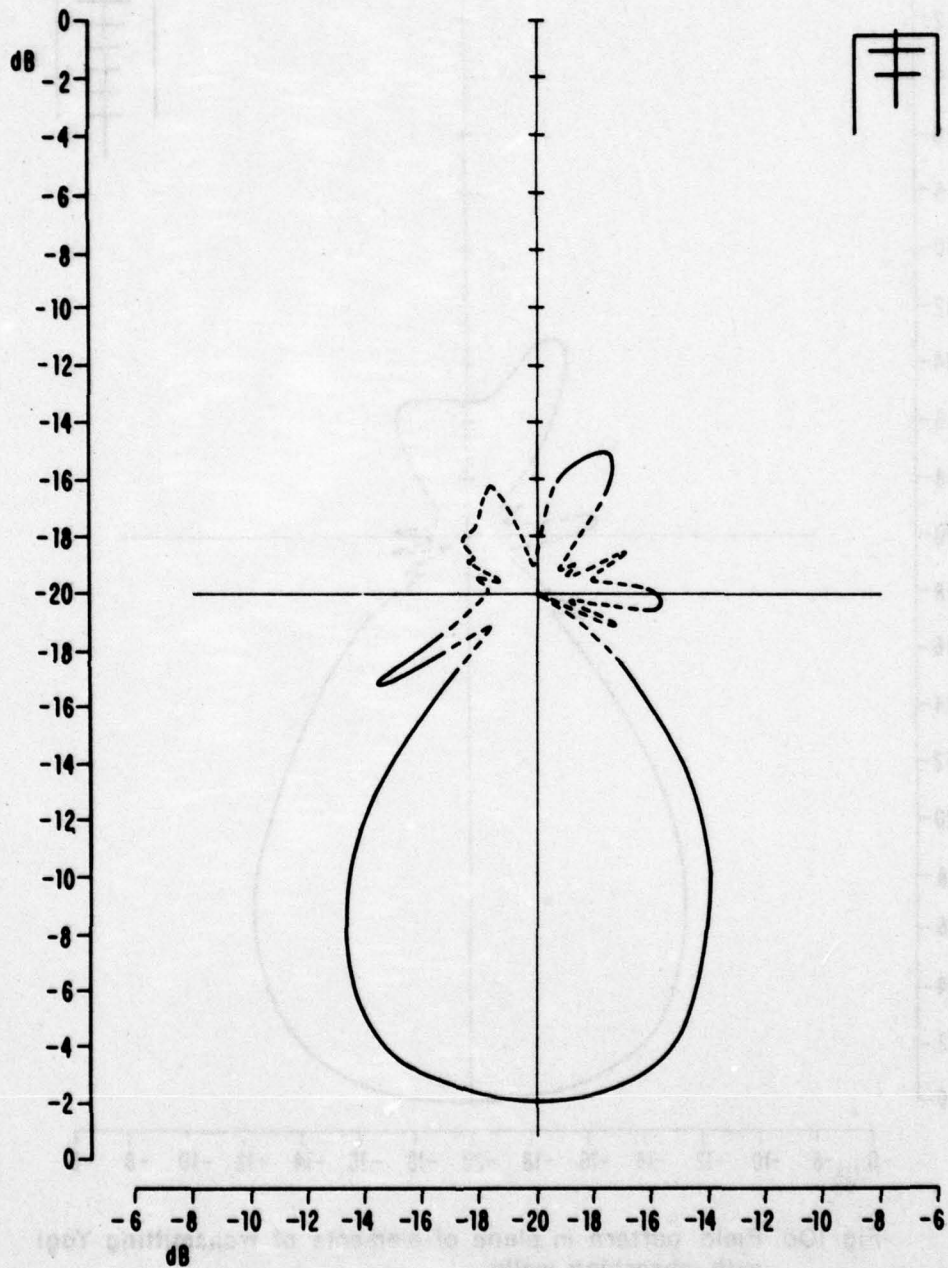


Fig. 10b Field pattern in plane of elements of receiving dipole with reflector with absorbing walls.

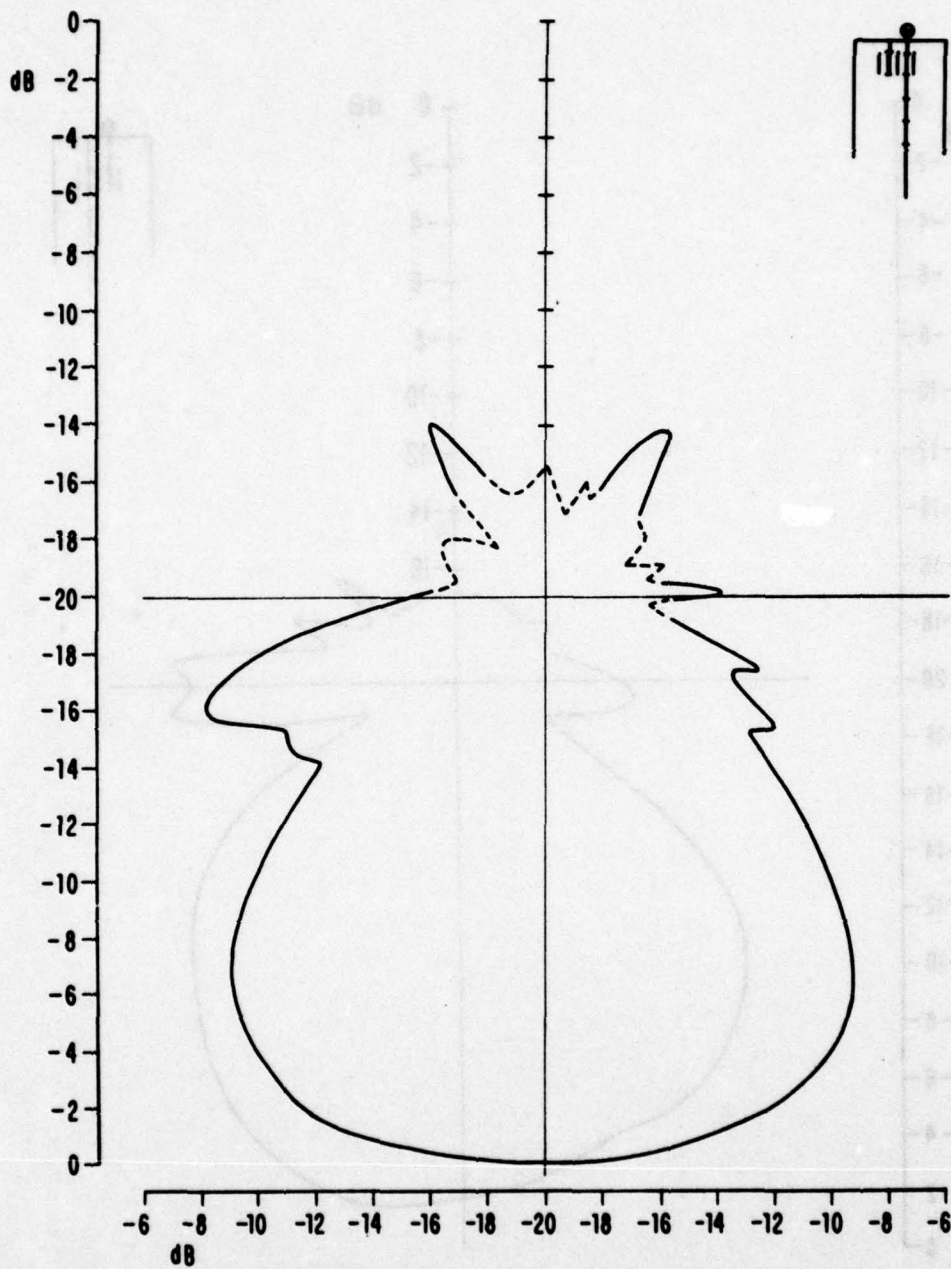


Fig. 10c Field pattern in plane bisecting elements of transmitting Yagi with absorbing walls.

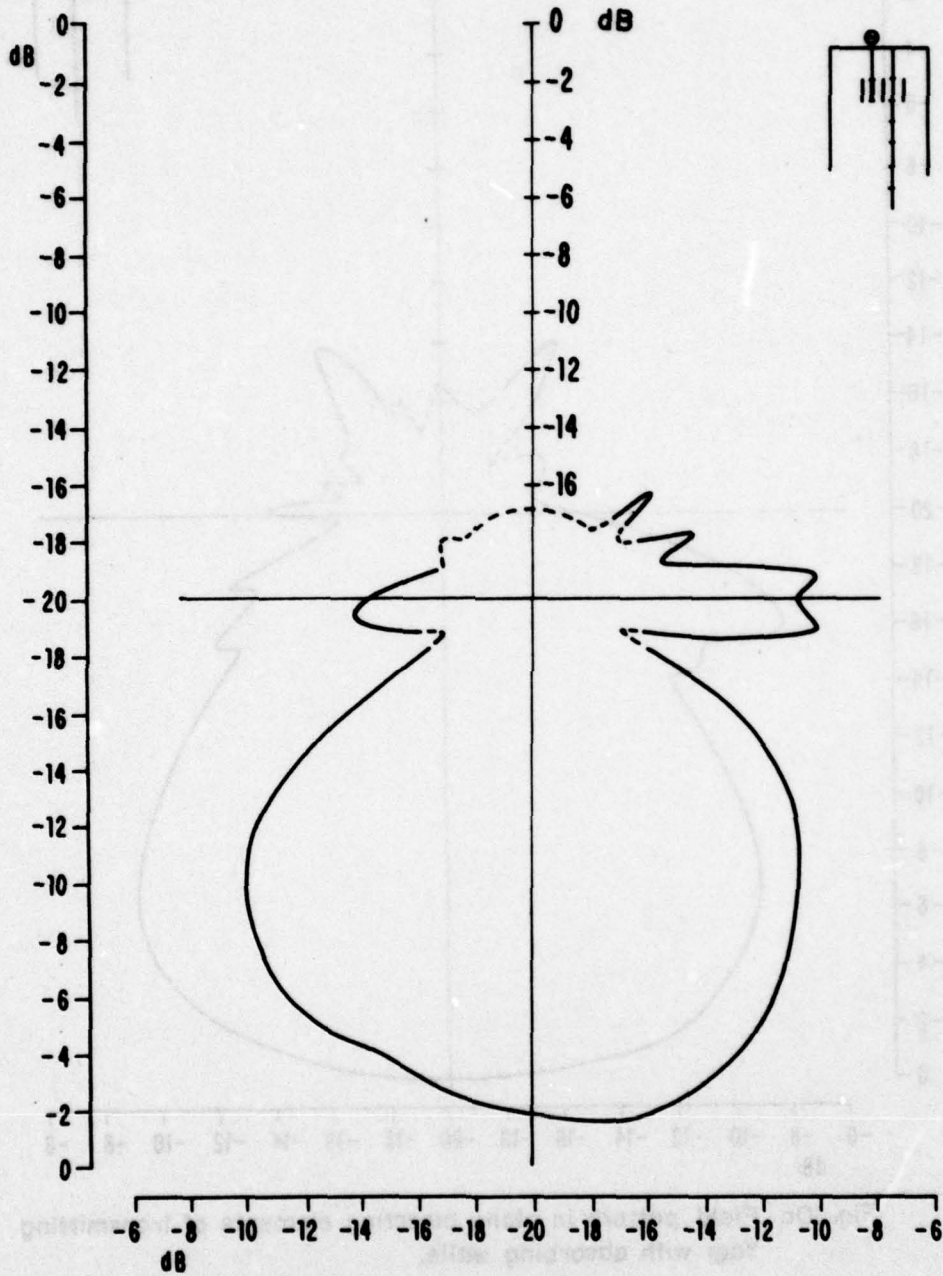


Fig. 10d Field pattern in plane bisecting elements of receiving antenna with absorbing walls.

PART II
THEORY OF SCATTERING FROM HORIZONTAL-WIRE ANTENNAS

2.1. Introduction

The problems associated with the scattering of electromagnetic waves by a wire at an arbitrary height d over the surface of the sea, a fresh-water lake, various types of soil and sand, or the arctic ice, are more readily understood if the driven horizontal-wire is studied first. This arises in part from the fact that the driven infinitesimal horizontal dipole near the plane interface between two electrically different half-spaces has been the subject of serious analytical study beginning with the work of Sommerfeld [6], [7], v. Hörschelmann [8], Weyl [9], Van der Pol and Niessen [10], Niessen [11], Van der Pol [12], and many others. A concise review of this early work is given by Bremmer [13]. It includes the exact theory and the related physical interpretations of the field of the horizontal electric dipole and of an arbitrary system of currents over the earth. More recent comprehensive work on dipoles over the earth is contained in a comprehensive volume by Baños [2], and in publications by Wait [14] and Chang [15].

2.2. Currents and Field of the Driven Horizontal-Wire Antenna Over the Earth

The infinitesimal dipole is a conveniently idealized source for studying the properties of electromagnetic waves in and in the presence of the earth or another material body, but it is not a practical antenna for point-to-point communication. For actual transmission, antennas of finite size with desirable and known characteristics both as circuit elements (admittance, current distribution) and as directional radiators (field pattern) are required. The analytical determination of these properties is difficult since they involve not only the shape and dimensions of the antenna, but also the conducting and dielectric properties of the earth or other body near which it is located or in which it is embedded. Evidently, the field generated by the currents in an antenna can be calculated from the known field of an infinitesimal dipole only after the distributions of current have been determined. The frequently used expedient of assuming a conveniently simple distribution is not generally

adequate.

An antenna for which an analytically determined distribution of current is available that takes full account of the electrical properties of an adjacent or surrounding material half-space is the horizontal wire, i.e., the wire parallel to the air-earth boundary at a height d above or below it. When located in the air above but quite close to the surface and provided with suitable terminations, it is the well-known Beverage wave antenna with its desirable directivity. In its original form it consisted of a wire several wavelengths long and only a very small fraction of a wavelength (e.g., 0.001λ) above the surface of the earth. Each end was grounded through a nonreflecting impedance of which one was the receiving load. Recently, antennas of this type have been considered as possible elements in extensive transmitting and receiving arrays erected near the surface of the earth for use as an over-the-horizon radar.

The current distribution along a horizontal-wire antenna at a height d above a material half-space (earth) depends in a complicated manner on the conductivity and permittivity of the material. Nevertheless, if the medium is electrically dense and the height of the antenna sufficiently small, the current distribution is formally relatively simple - actually simpler than when the same antenna is very far from the boundary. The explanation for this seemingly paradoxical observation is found in the fact that when the transfer of power into the material half-space greatly exceeds that radiated into the air and so dominates the distribution of current, this has the simple sinusoidal form that is characteristic of the transmission line. The loading effect of the adjacent conducting or dielectric medium is distributed uniformly along the antenna so that it can be included in the series impedance per unit length. The current distribution is then quite accurately sinusoidal with a complex wave number that depends on the effects of radiation and dissipation in the material medium. Radiation into the air, on the other hand, affects the distribution of current in a manner that does not permit its representation as a uniformly distributed load. The transmission-line properties of the horizontal-wire antenna and the conditions under which they are valid have been derived theoretically and verified experimentally by King et al. [16], and Sorbello et al. [17] for a single wire, and by Shen et

a1. [18] for coupled wires.

The theoretically derived solutions for the currents in horizontal-wire antennas apply specifically only when the wires are at an electrical height in air (region 2) given by $k_2 d \leq \pi/2$ over a material half-space (region 1) that is relatively dense. That is, the magnitude of the generally complex wave number $k_1 = \beta_1 + i\alpha_1 = \omega(\mu_0 \tilde{\epsilon}_1)^{1/2}$ is large compared with the real wave number $k_2 = \omega(\mu_0 \epsilon_0)^{1/2}$ of the air. In symbols, $|k_1/k_2|^2 \gg 1$. The complex permittivity of the material half-space is $\tilde{\epsilon}_1 = \epsilon_e + i\sigma_e/\omega$, where ϵ_e and σ_e are, respectively, the real effective permittivity and conductivity. The time dependence is $e^{-i\omega t}$. When these conditions are satisfied, the horizontal-wire antenna has all of the properties of a transmission line like that shown in Fig. 11(a). The complex wave number for the current is $k_L = \beta_L + i\alpha_L = (-z_L y_L)^{1/2}$ and the characteristic impedance is $Z_c = (z_L/y_L)^{1/2}$. Explicit formulas for k_L and Z_c as well as for the series impedance per unit length z_L and shunt admittance per unit length y_L are in [16] for the single wire. The formulas for k_L and Z_c are:

$$k_L = k_2 \{1 + [2/\ln(2d/a)] \{1/(2k_1 d)^2 - K_1(2k_1 d)/2k_1 d + i\pi I_1(2k_1 d)/4k_1 d - i(2k_1 d/3 + (2k_1 d)^3/45 + (2k_1 d)^5/1575 + \dots)\}\}^{1/2} \quad (1)$$

$$Z_c = (k_L \zeta_2 / 2\pi k_2) \cosh^{-1}(d/a) \pm (k_L \zeta_2 / 2\pi k_2) \ln(2d/a) \quad (2)$$

where $\zeta_2 = (\mu_0/\epsilon_0)^{1/2} \pm 120\pi$ ohms, K_1 and I_1 are the modified Bessel functions. Comparable formulas for coupled horizontal wires are in [18].

The general formula for the current at the point x along a horizontal wire, shown in Fig. 11(b), that extends from $x = 0$ (termination Z_0) to $x = s$ (termination Z_s) when driven by an emf V_u^e at $x = u$ is [19]:

$$I_x(x) = \frac{-iV_u^e \sin(k_L x + i\theta_0) \sin[k_L(s-u) + i\theta_s]}{Z_c \sin(k_L s + i\theta_0 + i\theta_s)} ; 0 \leq x \leq u \quad (3)$$

$$I_x(x) = \frac{-iV_u^e \sin(k_L u + i\theta_0) \sin[k_L(s-x) + i\theta_s]}{Z_c \sin(k_L s + i\theta_0 + i\theta_s)} ; u \leq x \leq s \quad (4)$$

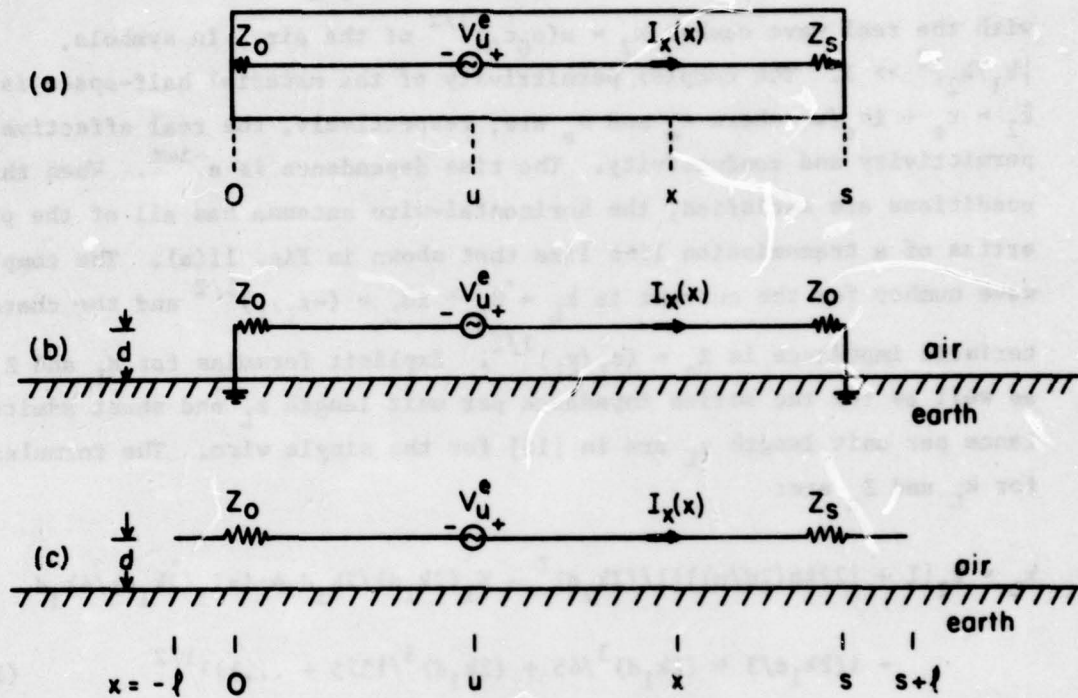


FIG. 11(a) COAXIAL LINE DRIVEN AT ARBITRARY POINT u AND TERMINATED IN IMPEDANCES AT EACH END. (b) ANALOGOUS HORIZONTAL WIRE WITH IMPEDANCES AT ENDS GROUNDED (BEVERAGE ANTENNA). (c) ANALOGOUS HORIZONTAL WIRE WITH IMPEDANCES AT ENDS CONNECTED TO MONOPOLES (GENERALIZED BEVERAGE ANTENNA).

The complex terminal functions are: $\theta_v = \rho_v - i\phi_v = \coth^{-1}(Z_v/Z_c)$, where $v = 0$ or s . The driving-point admittance is $Y_{in} = I_x(u)/V_u^e$. For a center-driven wire ($u = s/2$) with length $s = 2h$ and origin moved to the center with $x' = x - h$, these formulas give:

$$I_x(x') = \frac{-iv_0^e}{2Z_c} \frac{\sin[k_L(h - |x'|) + i\theta_s]}{\cos(k_L h + i\theta_s)} \quad (5)$$

when $\theta_0 = \theta_s$. When the ends of the antenna are open with no attached terminations or ground connections, $\theta_s = \rho_s - i\phi_s$ is nevertheless significant. In this case, ρ_s takes account of the relatively small radiation into the air and ϕ_s of a small capacitive end effect [17]. When the generator is located at $u = 0$ and $Z_0 = Z_s = Z_c$ in Fig. 11(b), the current in the conventional Beverage antenna has the simple form:

$$I_x(x) = \frac{v_0^e}{2Z_c} e^{ik_L x}, \quad 0 \leq x \leq s \quad (6)$$

In the generalized circuit in Fig. 11(c), the combined effective terminating impedance of Z_0 or Z_s and the impedance of the monopole with length $l \sim \lambda/4$ is chosen to be Z_c . In this case, the current in the range $0 \leq x \leq s$ is given by (6) and the currents in the two extensions are:

$$I_x(x) = I_x(0) \frac{\sin[k_L(l + x) + i\theta_0]}{\sin(k_L l + i\theta_0)}, \quad -l \leq x \leq 0 \quad (7)$$

$$I_x(x) = I_x(s) \frac{\sin[k_L(s + l - x) + i\theta_s]}{\sin[k_L(s + l) + i\theta_s]}, \quad s \leq x \leq s + l \quad (8)$$

where $I_x(0) = v_0^e/2Z_c$ and $I_x(s) = (v_0^e/2Z_c)e^{ik_L s}$. It is shown by direct measurement in [17] that Z_s and l for the monopole can be chosen so that (6) is an excellent representation of the current along the main part of the antenna between $x = 0$ and $x = s$. Note that the generalized form of the Beverage antenna shown in Fig. 11(c) is often preferable to the form with grounded ends shown in Fig. 11(b) since it does not depend on

ground connections which are practical only when the earth is quite highly conducting.

The electromagnetic field maintained in the air or the earth by the currents in the horizontal-wire antenna shown in Fig. 12 can be obtained by integration from the known field of an infinitesimal horizontal dipole with moment $I_x(x') dx'$. In the air above the earth the component of interest is usually E_z . This is generated by the vertically directed component of the currents induced in the earth. The field due to the element of current $I_x(x') dx'$ and the associated induced currents in the earth are given by Baños [2] in a compact form. When the indicated differentiation in Baños' formula is carried out, the result for the incremental E_{2z} is:

$$dE_{2z} = \frac{i\omega\mu_0}{4\pi k_2^2} I_x(x') dx' \cos \phi \int_0^\infty d\lambda \lambda^2 J_1(\lambda\rho) \left\{ \pm e^{i\gamma_2|d-z|} + \frac{k_2^2\gamma_1 - k_1^2\gamma_2}{k_2^2\gamma_1 + k_1^2\gamma_2} e^{i\gamma_2(d+z)} \right\} \quad (9)$$

where the upper sign is for $z > d$, the lower sign for $0 \leq z \leq d$. In (9), $\gamma_1^2 = (k_1^2 - \lambda^2)$ and $\gamma_2^2 = (k_2^2 - \lambda^2)$. The field due to the entire generalized wave antenna, shown in Fig. 11(c), is obtained by integration over its length. At radial distances ρ_0 from the origin that are great compared to the length $s + 2\ell$ of the antenna ($\rho \gg s + 2\ell$), $\rho \approx \rho_0 - x' \cos \phi_0$ and

$$E_{2z} = \frac{i\omega\mu_0 V_0^e}{8\pi^2 k_2^2 Z_c} \cos \phi_0 \left\{ \int_0^s dx' e^{ik_L x'} F(x') + \int_{-\ell}^0 dx' \frac{\sin[k_L(\ell + x') + i\theta_2]}{\sin(k_L \ell + i\theta_2)} \times F(x') + e^{ik_L s} \int_s^{s+\ell} dx' \frac{\sin[k_L(\ell - x') + i\theta_2]}{\sin(k_L \ell + i\theta_2)} F(x') \right\} \quad (10)$$

where

$$F(x') = \int_0^\infty d\lambda \lambda^2 J_1[(\rho_0 - x' \cos \phi_0)\lambda] \left\{ \pm e^{i\gamma_2|d-z|} + \frac{k_2^2\gamma_1 - k_1^2\gamma_2}{k_2^2\gamma_1 + k_1^2\gamma_2} e^{i\gamma_2(d+z)} \right\} \quad (11)$$

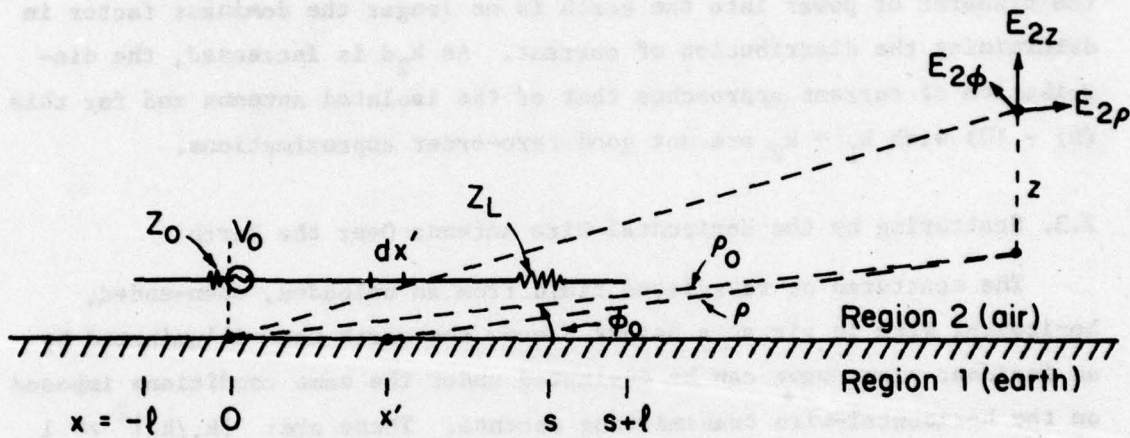


FIG.12 GENERALIZED WAVE ANTENNA AT HEIGHT d OVER A PLANE EARTH

is proportional to the field of an infinitesimal dipole at x' . In (10), E_{2z} is the complete formula for the vertical component of the electric far field at a height z above the earth due to the current in a horizontal wave antenna at the radial distance ρ_0 and at the height d above the earth. It takes full account of the effect of the earth on the current and on the field. The conditions $|k_1/k_2|^2 \gg 1$ and $k_2 d \leq \pi/2$ must be satisfied. At heights $k_2 d > \pi/2$ the simple sinusoidal form of the current with a complex wave number k_L is not an adequate approximation since the transfer of power into the earth is no longer the dominant factor in determining the distribution of current. As $k_2 d$ is increased, the distribution of current approaches that of the isolated antenna and for this (6) - (8) with $k_L \rightarrow k_2$ are not good zero-order approximations.

2.3. Scattering by the Horizontal-Wire Antenna Over the Earth

The scattered or reradiated field from an unloaded, open-ended, horizontal wire in air at a height d over the earth when illuminated by an incident plane wave can be evaluated under the same conditions imposed on the horizontal-wire transmitting antenna. These are: $|k_1/k_2|^2 \gg 1$ and $k_2 d \leq \pi/2$. The current induced in the scattering antenna is that due to a continuous distributions of generators along its entire length with amplitude and phase at each point $x = u$ equal to that of the tangential component of the incident electric field at that point. That is, the current in the wire due to the incident field acting at $x = u$ over the incremental length du is given by (3) and (4) with $V_u^e = E_{\text{tang}}^{\text{inc}} du$. Consider for simplicity that the wire is oriented for maximum scattering with its axis in the plane wave front of the incident field parallel to the electric vector as shown in Fig. 13. It is at a height d above the earth, perpendicular to the plane of incidence, $x = 0$. The propagation vector \hat{k}_2 of the incident wave is perpendicular to the wire but an arbitrary angle θ_1 with respect to the vertical z -axis. Under these conditions, the total incident field acting to induce currents in the wire includes both direct and reflected components. This latter is determined by the plane-wave reflection coefficient f_{mr} for which the magnetic vector is in the plane of incidence as in Fig. 13. The total field acting to induce currents in the wire is:

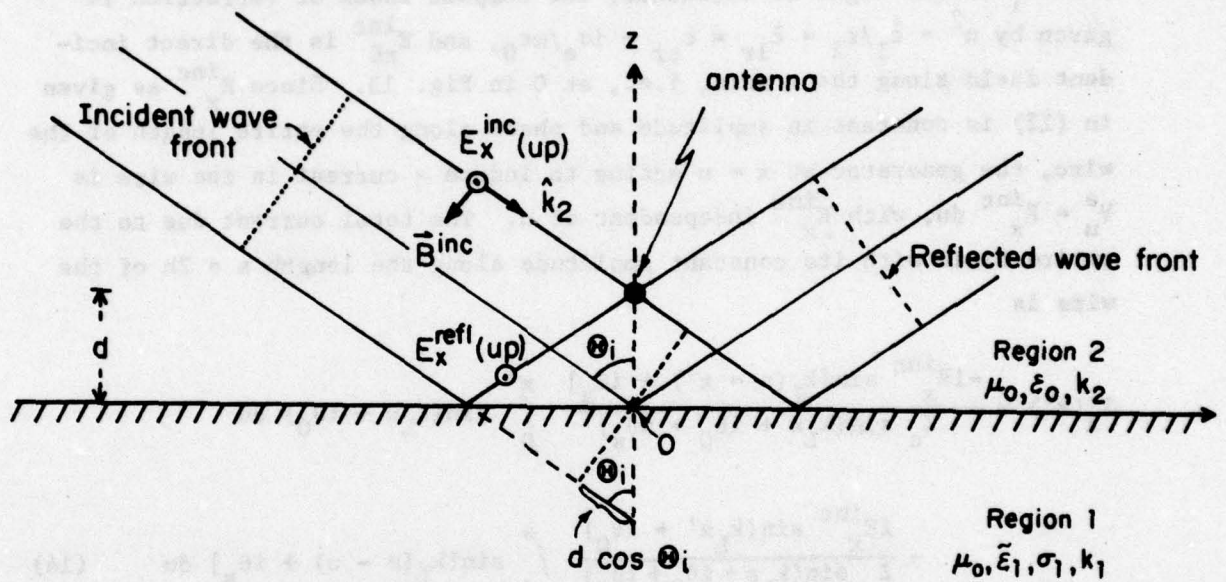


FIG.13 HORIZONTAL WIRE AS SCATTERING ANTENNA

$$E_x^{inc} = E_{x0}^{inc} \left(e^{-ik_2 d \cos \theta_1} + f_{mr} e^{ik_2 d \cos \theta_1} \right) \quad (12)$$

with

$$f_{mr} = \frac{n \cos \theta_1 - (1 - n^2 \sin^2 \theta_1)^{1/2}}{n \cos \theta_1 + (1 - n^2 \sin^2 \theta_1)^{1/2}} \quad (13)$$

Here θ_1 is the angle of incidence, the complex index of refraction is given by $n^2 = \tilde{\epsilon}_1/\epsilon_2 = \tilde{\epsilon}_{1r} = \epsilon_{er} + i\sigma_e/\omega\epsilon_0$, and E_{x0}^{inc} is the direct incident field along the x axis, i.e., at 0 in Fig. 13. Since E_x^{inc} as given in (12) is constant in amplitude and phase along the entire length of the wire, the generator at $x = u$ acting to induce a current in the wire is $V_u^e = E_x^{inc} du$, with E_x^{inc} independent of u . The total current due to the entire field with its constant amplitude along the length $s = 2h$ of the wire is

$$I_x(x') = \frac{-iE_x^{inc} \sin[k_L(s - x') + i\theta_s]}{Z_c \sin(k_L s + i\theta_0 + i\theta_s)} \int_0^{x'} \sin(k_L u + i\theta_0) du - \frac{iE_x^{inc} \sin(k_L x' + i\theta_0)}{Z_c \sin(k_L s + i\theta_0 + i\theta_s)} \int_{x'}^s \sin[k_L(s - u) + i\theta_s] du \quad (14)$$

This is readily integrated. If the origin of coordinates is moved to the center of the wire with the substitutions $x' = x - h$, $s = 2h$, and the ends are assumed to be identical, i.e., $Z_0 = Z_s = Z_h$, $\theta_0 = \theta_s = \theta_h$, the induced current is given by:

$$I_x(x) = \frac{-iE_x^{inc}}{k_L Z_c} \left[\frac{\cos k_L x \cos \theta_h - \cos(k_L h + i\theta_h)}{\cos(k_L h + i\theta_h)} \right] \quad (15)$$

With (12) and (13), this is the final formula for the induced current at a distance x from the center of a horizontal wire with the length $s = 2h$ and at a height d over the earth, when terminated at each end in the impedance $Z_h = Z_c \coth \theta_h$. The usual scattering wire has open ends for which $\theta_h = \rho_h - i\theta_h$ has small values that take account of the capacitive

end effect (in ϕ_h) and reradiation into the air (in ρ_h). When $k_2 d$ is small, $\theta_h \approx 0$ and (15) reduces to:

$$I_x(x) = \frac{-iE_x^{inc}}{k_L Z_c} \left[\frac{\cos k_L x - \cos k_L h}{\cos k_L h} \right] \quad (16)$$

Actually, the effect on the distribution of current of the terms in h in (15) is not great when the assumed condition $k_2 d \leq \pi/2$ is satisfied. In fact, the distribution $I_x(x) = I_x(0)(\cos k_L x - \cos k_L h)/(1 - \cos k_L h)$ is a good zero-order approximation even when $d \rightarrow \infty$ and $k_L \rightarrow k_2$. However, the characteristic impedance Z_c in (16) cannot be used as defined in [16] when $k_2 d > \pi/2$.

The largest and most important component of the scattered field is E_{2x}^{scat} on and perpendicular to the plane $x = 0$, as shown in Figs. 13 and 14. In the cylindrical coordinates (ρ, ϕ, z) with origin on the surface of the earth below the center of the antenna, the plane $x = 0$ corresponds to $\phi = \pi/2, 3\pi/2$, as shown in Fig. 15. The reradiated or scattered field at the point $(x = 0, y = \rho = R_0 \sin \theta, z = R_0 \cos \theta)$ shown in Fig. 14 and due to the current element $I_x(x') dx'$ at $x = x'$ in the wire is readily obtained from the formulas given by Baños [2]. Thus,

$$dE_{2\phi}^{scat}(\phi = \pi/2) = dE_{2x}^{scat} = I_x(x') dx' F_{2x} \quad (17)$$

where

$$F_{2x} = \frac{\omega\mu_0}{4\pi k_2^2} \left(\int_0^\infty d\lambda \lambda \frac{e^{i\gamma_2|d-z|}}{\gamma_2} \{k_2^2 J_0(\lambda\rho) - (\lambda^2/2)[J_0(\lambda\rho) + J_2(\lambda\rho)]\} \right. \\ \left. + (1/2) \int_0^\infty d\lambda \lambda e^{i\gamma_2(d+z)} \left\{ \frac{k_2^2(\gamma_2 - \gamma_1)}{\gamma_2(\gamma_2 + \gamma_1)} + \gamma_2 \left(\frac{k_2^2\gamma_1 - k_1^2\gamma_2}{k_2^2\gamma_1 + k_1^2\gamma_2} \right) \right\} J_0(\lambda\rho) \right. \\ \left. + (1/2) \int_0^\infty d\lambda \lambda^3 e^{i\gamma_2(d+z)} \left\{ \frac{1}{\gamma_2} - \frac{2k_2^2}{k_2^2\gamma_1 + k_1^2\gamma_2} \right\} J_2(\lambda\rho) \right) \quad (18)$$

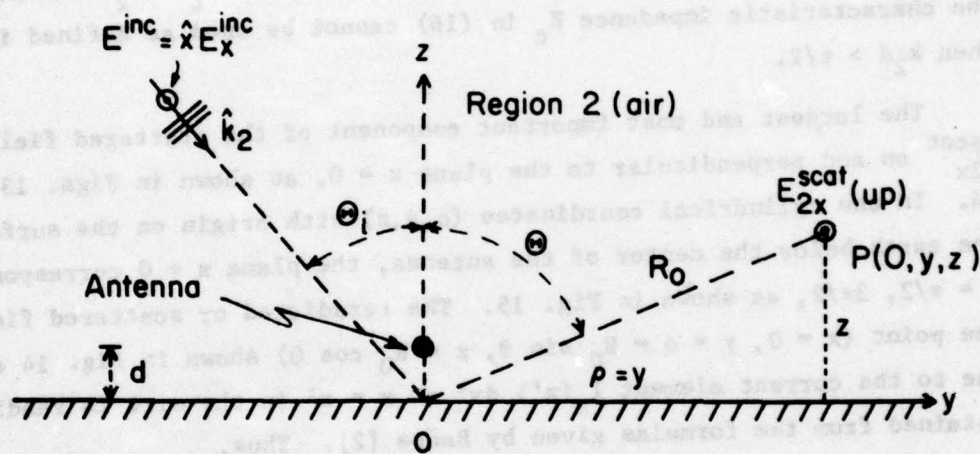


FIG.14 HORIZONTAL WIRE IN PRESENCE OF MATERIAL HALF SPACE AS SCATTERING ANTENNA

is the field of a unit dipole moment. In (18), $\rho = R_0 \cos \theta$ and $z = R_0 \sin \theta$, where θ is the angle of observation and R_0 the distance from the origin on the boundary to the point of observation. As before, $\gamma_1^2 = k_1^2 - \lambda^2$, $\gamma_2^2 = k_2^2 - \lambda^2$. The scattered far field at any sufficiently distant point in the plane $x = 0$ is readily obtained since such a point is equidistant from all elements of current in the reradiating conductor. Thus, when (15) is substituted in (17) and this is integrated over the length of the conductor, the variable of integration occurs only in the current and the total field is:

$$E_{2x}^{\text{scat}} = \frac{-2iE_x^{\text{inc}}}{k_L^2 Z_c} \left[\frac{\sin k_L h \cos i\theta_h - k_L h \cos(k_L h + i\theta_h)}{\cos(k_L h + i\theta_h)} \right] F_{2x} \quad (19)$$

In (19), E_x^{inc} is the total x-component of the incident field given by (12) with (13) and F_{2x} is the field per unit dipole moment given by (18). If θ_h is neglected, the trigonometric factor in (19) reduces simply to $(\tan k_L h - k_L h)$, where $k_L = \beta_L + i\alpha_L$ is, of course, complex. E_{2x}^{scat} in (19) is the total scattered field in the plane $x = 0$ of a horizontal wire with length $2h$ at an electrical height $k_2 d \leq \pi/2$ over a matter-filled half-space with $|k_1^2/k_2^2| \gg 1$. The other components of the scattered field and the field at points other than in the plane $x = 0$ can be obtained in the same general manner. The function F_{2x} in (18) has been evaluated by King and Sandler [20] for the infinitesimal dipole over wide ranges of the parameters.

2.4. Conclusion

The general formulas for the electromagnetic field of a horizontal infinitesimal dipole over a dielectric or conducting half-space as given by Bremner [13], Baños [2], and others have been combined with the currents derived by King et al. [16] for the distributions of current along practical antennas near and in the half-space to obtain the far fields. Two antennas for which the currents are known in their dependence on the properties of the material half-space have been treated. These are the generalized Beverage wave antenna as a transmitter, and the horizontal-wire antenna as a scatterer in the presence of the half-space.

REFERENCES

- [1] J. R. Wait, Guest Editor, IEEE Trans. Antennas Propagat., Special Issue on Electromagnetic Waves in the Earth, vol. AP-11, May 1963.
- [2] A. Baños, Jr., Dipole Radiation in the Presence of a Conducting Half-Space. Oxford, England: Pergamon Press, 1966.
- [3] E. J. Blun and M. J. Lun, "Electromagnetic Wave Propagation in Conducting Media, an Annotated Bibliography," TG-230-B6, APL Library Bulletin, Bibliography Services, The John Hopkins University Applied Physics Laboratory, Silver Springs, Maryland, September 1966.
- [4] T. T. Wu, "Theory of the Thin Circular Loop Antenna," J. Math. Phys., vol. 3, pp. 1301-1304, Nov.-Dec. 1962.
- [5] R. W. P. King, R. B. Mack, and S. S. Sandler, Arrays of Cylindrical Dipoles. New York: Cambridge University Press, 1968.
- [6] A. Sommerfeld, "Ueber die Ausbreitung der Wellen in der drahtlosen Telegraphie," Ann. Physik, vol. 28, p. 665, 1909.
- [7] A. Sommerfeld, "Ueber die Ausbreitung der Wellen in der drahtlosen Telegraphie," Ann. Physik, vol. 81, p. 1135, 1926.
- [8] H. v. Hörschelmann, "Ueber die Wirkungsweise des geknickten Marconischen Senders in der drahtlosen Telegraphie," Jahrb. draht. Tel. u. Tel., vol. 5, pp. 14 and 188, 1912.
- [9] H. Weyl, "Ausbreitung elektromagnetischer Wellen über einem ebenen Leiter," Ann. Physik, vol. 60, p. 481, 1919.
- [10] B. Van der Pol and K. F. Niessen, "Ueber die Raumwellen von einem vertikalen Dipolsender auf ebener Erde," Ann. Physik, vol. 10, p. 485, 1931.
- [11] K. F. Niessen, "Erdabsorption bei horizontalen Dipolantennen," Ann. Physik, vol. 32, p. 444, 1938.
- [12] B. Van der Pol, "Theory of the Reflection of Light from a Point Source by a Finitely Conducting Flat Mirror, with an Application to Radiotelegraphy," Physica, vol. 2, pp. 843-853, 1935.
- [13] H. Bremmer, "Propagation of Electromagnetic Waves," Part IV in S. Flügge, Encyclopedia of Physics, Vol. 16. Berlin: Springer-Verlag, 1958.
- [14] J. R. Wait, Chapters 23 and 24 in Antenna Theory, Part II, R. E. Collin and F. J. Zucker, Eds. New York: McGraw-Hill, 1969.
- [15] D. C. Chang, Chapter 7 in Electromagnetic Probing in Geophysics, J. R. Wait, Ed. Boulder, Colorado: Golem Press, 1971.

- [16] R. W. P. King, L. C. Shen, and T. T. Wu, "The Horizontal-Wire Antenna Over a Conducting or Dielectric Half-Space: Current and Admittance," Radio Science, vol. 9, pp. 701-709, 1974.
- [17] R. M. Sorbello, R. W. P. King, K.-M. Lee, L. C. Shen, and T. T. Wu, "The Horizontal-Wire Antenna Over a Dissipative Half-Space: Generalized Formula and Measurements," IEEE Trans. Antennas Propagat., vol. AP-25, pp. 850-854, 1977.
- [18] L. C. Shen, K.-M. Lee, and R. W. P. King, "Coupled Horizontal-Wire Antennas Over a Conducting or Dielectric Half-Space," Radio Science, vol. 12, pp. 687-698, 1977.
- [19] R. W. P. King, Transmission-Line Theory. New York: Dover, 1965, pp. 245-246.
- [20] R. W. P. King and B. H. Sandler, "Subsurface Communication Between Dipoles in General Media," IEEE Trans. Antennas Propagat., vol. AP-25, pp. 770-775, 1977.

MISSION
of
Rome Air Development Center

RADC plans and executes research, development, test and selected acquisition programs in support of Command, Control Communications and Intelligence (C³I) activities. Technical and engineering support within areas of technical competence is provided to ESD Program Offices (POs) and other ESD elements. The principal technical mission areas are communications, electromagnetic guidance and control, surveillance of ground and aerospace objects, intelligence data collection and handling, information system technology, ionospheric propagation, solid state sciences, microwave physics and electronic reliability, maintainability and compatibility.